2015

Development of dielectric spectroscopic sensor for contaminant detection in a hydraulic fluid and a compressed air stream

Safal Kshetri
Iowa State University

Development of dielectric spectroscopic sensor for contaminant detection in a hydraulic fluid and a compressed air stream

by

Safal Kshetri

A thesis submitted to the graduate faculty

in partial fulfillment of the requirements for the degree of

MASTER OF SCIENCE

Major: Agricultural and Biosystems Engineering

Program of Study Committee:
Brian Steward, Major Professor
Stuart Birrell
Steven Hoff

Iowa State University

Ames, Iowa

2015

DEDICATION

To my family and friends

TABLE OF CONTENTS

LIST OF FIGURES

LIST OF TABLES

ACKNOWLEDGMENTS

First and foremost, I would like to express my sincere gratitude to my advisor Dr. Brian Steward for his patience, motivation, knowledge and valuable suggestions throughout the research. His continuous guidance has helped me become more disciplined and organized in my work. He has been a great mentor and I appreciate his willingness to help whenever I was in need.

I am also grateful to Dr. Stuart Birrell for his insightful comments and suggestions during my research. I have learned a lot from his vast knowledge and skills. I would also like to express my gratitude to Dr. Steven Hoff for his valuable suggestions to improve my thesis. I greatly admire his enthusiasm in teaching, which has been instrumental in strengthening my knowledge on mechatronics and augmented my interest on the subject.

I must acknowledge my colleagues Augusto D'Souza, Katherine Hinkle, Jafni Jiken, Dillon Wirth, Kenneth Mapoka, Wyatt Hall, Matt Schramm and Manish Shrivastav for their continuous support and creating a work environment that brought the best out of me. Special thanks go to the National Fluid Power Association, whose generous support for the research helped me continue my academic pursuit and enhance my skills that are essential for my successful career.

Finally, my sincerest thanks go to all the staff members of Department of Agricultural and Biosystems Engineering for their generous help and support.

ABSTRACT

A change in a fluid's dielectric properties can be investigated using dielectric spectroscopy to gain valuable insight into the changing condition of the fluid. A dielectric spectroscopic sensor was developed using a cylindrical capacitive sensing unit with the fluid as the dielectric media. The sensor was used to estimate or detect contaminants in a hydraulic fluid and a compressed air stream. Tests were performed with a hydraulic fluid in which the dielectric sensor's performance was evaluated in detecting iron powder and ISO medium test dust particles as contaminants in the fluid. Using iron powder as contaminants, two tests were performed with central electrodes of diameters 6.35 mm and 17.7 mm inch placed inside the capacitive dielectric sensor. The results from partial least squares (PLS) regression showed that the root mean square error of calibration (RMSEC) and the root mean square error of cross-validation (RMSECV) for a 6.35 mm (0.25-inch) diameter central electrode were 1.1 and 1.39 of adjusted ISO cleanliness code respectively. For a 17.7 mm (0.70-inch) diameter central electrode, the RMSEC and RMSECV values were 0.62 and 0.83 of adjusted ISO cleanliness code, respectively. Similarly, a test was performed using ISO test dust particles as contaminants with a central electrode of 17.7 mm diameter. The RMSEC and RMSECV values from the model for ISO test dust were 1.29 and 1.48 of adjusted ISO cleanliness code, respectively. Tests were also conducted to investigate the efficacy of dielectric spectroscopy in detecting water and oil droplets in a compressed air stream. Spray nozzles were used to produce fine droplets of deionized water and light lubricant oil. Multivariate statistical techniques, principal component analysis (PCA) and linear discriminant analysis (LDA), were used to develop statistical classifiers, which determined the performance of dielectric spectroscopic sensor in differentiating the dry

compressed air from an air stream with entrained liquid droplets. Through model calibration and cross-validation, the classifiers were able to separate the two cases without any errors, validating the dielectric sensor's ability to detect of liquid droplets in an air stream.

CHAPTER 1. INTRODUCTION

Hydraulic fluids and compressed air, based on their usability, have been widely used for power transmission and control as well as motion control in a variety of fluid power applications. These applications make the fluid power a very important part of agriculture, construction, transportation and manufacturing industries. According to the U.S. Census Bureau, sales of fluid power components and systems using fluid power exceeded $17.7B and $226B, respectively, in the USA in 2008 (Love et al., 2012). These sales reflect the importance of fluid power systems and components in modern industries.

Despite their importance, fluids are susceptible to contamination which causes many problems. Many modern hydraulic and pneumatic systems require high quality and clean fluid for reliable and efficient operation. However, these fluids become contaminated during normal operation of these systems. Thus systems for fluid conditioning and quality management must be designed into any fluid power system. The contaminants not only reduce efficiency of hydraulic and pneumatic components but also lead to catastrophic failure of these systems. Research has shown that about 70% of all failures in hydraulic systems are due to contaminants in the hydraulic fluid (Singh et al., 2012). This deleterious effect of contamination greatly increases the expense of maintenance and replacement of fluid power systems. For example, in some heavy manufacturing industries, maintenance can be as high as 40% of the total costs of the operation (Wang et al., 2012).

Increases in the contaminant levels and changes in fluid properties can be both indicators of deteriorating component conditions and cause of component failure (DTI, 1984; Cunningham, 1987; Troyer and Lazzeroni, 1994; Ashley, 1996). Low cost sensors capable of

providing early warnings of fluid problems by measuring changes in fluid properties could add significant value to hydraulic and pneumatic systems by providing an opportunity to take corrective action prior to failure. Measurement of viscosity, refractive index, density, base number (BN), acid number (AN), water content, metals (additive and wear metals), color, and flash point are some examples of common sensing techniques used to determine condition of the hydraulic fluid (Pérez and Hadfield, 2011).

Measuring changes in dielectric properties of the fluid can also provide information on the condition of the working fluid. Changes in the dielectric constant have been correlated with the presence of contaminants, such as water or particles, or changes in chemistry of the oil such as additive depletion or oxidation (Carey and Hayzen, 2001). Furthermore, these properties can be measured at several frequencies using a technique called dielectric spectroscopy (Von Hippel, 1954a). This technique has advantages over conventional sensing techniques. Most sensors acquire only a few measurements of various physical properties and try to predict contaminant levels (Sommers, 1997; Verdegan, 2010; McAdoo et al., 1998; Codina et al., 1997). The limitation of these conventional approaches is that there simply is not enough data required for robustness. Dielectric spectroscopic measurement addresses this problem by measuring the same condition of the fluid at different frequencies. A good knowledge of spectral data could provide a more accurate assessment of fluid condition.

Dielectric spectroscopy has been used for comparing different petroleum fractions (Folgero, 1998; Tjomsland, et al., 1996), sensing moisture dynamics in oil impregnated pressboard (Sheiretov and Zahn, 1995), and monitoring moisture content and insulation degradation in oil transformers (Koch and Feser, 2004). Some real-time oil sensors, such as the Kavlico Oil Quality Sensor and Lubrigard® Dielectric Sensor have been developed based

on dielectric measurements (Carey and Hayzen, 2001, Gebarin, 2003). The Delphi Diesel Engine Condition monitoring sensor under development is partly based on dielectric measurements in the 2-5 MHz Range (Wang et al., 1997; Wang, 2002). Bosch Ford (Saloka, 1991) and Hella (Wullner et al., 2003) have also reported on the development of oil conditioning monitoring systems based on dielectric methods.

For over a decade at Iowa State University, work in the dielectric spectroscopic sensing area has been carried out. This technology was used to sense physical properties of biomaterials (Al-Mahasneh et al., 2001; Eubanks and Birrell, 2001). In addition, Chighladze et al. (2010) documented the sensitivity of soil moisture probes to nitrate ions in soil solutions using dielectric measurements. Benning et al. (2004) developed a sensor that acquired dielectric measurements at four frequencies through a custom developed electrical circuit. The concept behind this work is that multiple frequency dielectric measurements provide “multiple equations” that could be used to separate the dielectric response due to the parameter of interest, from the dielectric response of other interference parameters. Aziz et al. (2007, 2009) also documented good performance in predicting water, metal, and dust contaminant levels in hydraulic fluids. These experiments were performed using a laboratory impedance analyzer to demonstrate proof-of-concept.

A well-designed dielectric spectroscopic sensor capable of taking in-line, vehicle-based measurements can have high economical value. For example, determining the quality of oil by measuring fluid properties usually requires collecting samples and using complex laboratory equipment (Carey and Hayzen, 2001). This approach is costly because of the expensive laboratory equipment and downtime associated with the sampling process. An inexpensive practical dielectric sensor, capable of early detection of contaminants, will not

only help minimize these expenses, but also help operators take necessary measures before any catastrophic system failure.

Objectives of the Research

The goal of the research was to develop a dielectric sensor and investigate its performance in the application of dielectric spectroscopy to:

1) measuring levels of particulate contaminants (iron powder and ISO test dust) in hydraulic fluid based on the ISO cleanliness code (ISO 4406:1999), and
2) detect the presence of typical contaminants, particularly water droplets, and lubricating oil droplets, in compressed air.

Thesis Organization

Chapter 2 describes in detail the theory behind dielectric properties and their relationship to dielectric spectroscopy. This chapter also details different important design aspects that were implemented in the dielectric sensor to enhance its performance. Chapter 3 is a journal article describing research investigating dielectric sensing in hydraulics, in which the performance of the dielectric sensor in the measurement of solid contaminants was documented. This chapter describes the construction of the dielectric sensor in more detail. Chapter 4 is another journal article outlining research exploring dielectric sensing of liquid aerosols in an air stream. Chapter 5 summarizes conclusions from the research and recommendations for future work. References for the content of each chapter are given at the end of the individual chapters. Appendix contains the drawings of the dielectric spectroscopic sensor that was developed in the research.

REFERENCES

Al-Mahasneh, M. A., S. J. Birrell, C. J. Bern, and K. Adam. 2001. Measurement of corn mechanical damage using dielectric properties. ASAE Paper N. 01-1073. ASABE, St. Joseph, Mich.

Ashley, S. 1996. Analyzing fluid contamination. Mechanical Engineering 118(4): 28-29.

Aziz, S. A., B. L. Steward, and S. J. Birrell. 2007. Dielectric spectroscopy of hydraulic fluid for contamination detection. In Proceedings of ISFP'2007: 5th International Symposium on Fluid Power Transmission and Control, Beidaihe, China, June 6-8.

Aziz, S. A., B. L. Steward, S. J. Birrell. 2009. Multifrequency dielectric sensing for hydraulic fluid contamination detection. NFPA Fall Conference, Wheeling, IL.

Benning, R., S. Birrell, and R. Gieger. 2004. Development of a Multi-Frequency Dielectric Sensing System for Real-Time Forage Moisture Measurement. ASAE Paper N. 04-1100. ASABE, St. Joseph, Mich.

Carey, A. A., and Hayzen, A. J. 2001. The Dielectric Constant and Oil Analysis. Retrieved May 16, 2014, from http://www.machinerylubrication.com/Read/226/dielectric-constant-oil-analysis

Chighladze, G., A. Kalieta, and S. Birrell. 2010. Sensitivity of Capacitance Soil Moisture Sensors to Nitrate Ions in Soil Solution. Soil Sci. Soc. Am. J. doi:10.2136/sssaj20010.0074.

Codina, G., C. Ramamoorthy, and D. J. Murr. 1997. Capacitive particle sensor. U.S. Patent 5,668,309.

Cunningham, E. R. 1987. Cleaning hydraulic fluids. Plant Engineering. June 11: 28.

Department of Trade and Industry. 1984. Contamination control in fluid power systems 1980-1983. Vol VIII Contamination Sensitivity - Standard Test Methods. East Kilbride, Glasgow, UK: Dept. of Trade and Industry.

Eubanks, J. C. and S. J. Birrell. 2001. Determining moisture content of hay and forages using multiple frequency ASAE Paper N. 01-1072. ASABE, St. Joseph, Mich.

Gebarin, S. 2003. On-line and In-line Wear Debris Detectors: What's Out There? Practicing Oil Analysis Magazine. September 2003.

Love, J. L., Lanke, E., and Alles, P., 2012. Estimating the Impact (Energy Emissions and Economics) of the U.S. Fluid Power Industry. Oak Ridge National Laboratory, pp. 5-6.

McAdoo, J. H., W. Catoe, M. W. Bollen, V. Fofen, and F. Volkening. 1998. Lubricating fluid condition monitoring. U.S. Patent 5754055.

Pérez, A. T., and Hadfield, M. 2011. Low-Cost Oil Quality Sensor Based on Changes in Complex Permittivity. *Sensors (Basel, Switzerland)*, *11*(11), 10675–10690.

Saloka, G.S., and A.H. Meitzler. 1991. Capacitive oil deterioration sensor. In: Proc. Society of Automotive Engineers, n P-242, Sensors and Actuators. p 137-146.

Sommers, H. T. 1997. Contamination Sensor. US Patent No. 5,939,727.

Troyer, D. D. and L. K. Lazzeroni. 1994. For quality sake, maintain hydraulic machines. Quality Progress 27(10): 91-96.

Verdegan, B. M. 2010. Combination contaminant size and nature sensing system and method for diagnosing contamination issues in fluids. US Patent 7,788,969.

Wang, S. S. 2002. Engine oil condition sensor: method for establishing correlation with total acid number. Sensors and Actuators B: Chemical 86(2-3): 122-26.

Wang, S. S., H. S. Lee, and D. J. Smolenski, 1997. The development of in situ electrochemical oil-condition sensors. Sensors and Actuators: B Chemical 17(3): 179-85.

Wang, Y., Zhang, M., and Liu, D. (2012). A Compact on-Line Particle Counter Sensor for Hydraulic Oil Contamination Detection. AMM Applied Mechanics and Materials, 130-134, 4198-4201.

Wüllner, D., H. Müller, O. Lüdtke, H. Dobrinski, and T. Eggers. 2003. Multi-functional Microsensor for Oil Condition Monitoring Systems Retrieved. In: 7th International Conference on Advanced Microsystems for Automotive Applications May 22-23, 2003, Berlin, p315.

CHAPTER 2. THEORY

Background

The dielectric sensor developed in the research used a cylindrical capacitive sensing unit in which the fluid under test passed between the coaxially arranged electrodes and served as the dielectric material. The cylindrical capacitor consists of two conducting cylinders of unequal diameter placed concentric to each other and separated by this dielectric material (Figure 1).

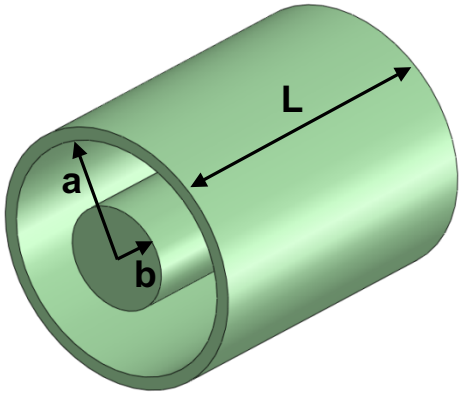

Figure 1. A cylindrical capacitor consists of two cylindrical conductors, the outer conductor with inner diameter a, and the inner conductor with outer diameter b.

The cylindrical capacitor can store electrical charge, and this ability to store charge is measured in terms of capacitance. Capacitance is the ratio of charge stored to voltage applied, or mathematically:

$$C = \frac{Q}{V} \tag{1}$$

where C is the capacitance in Farads,

Q is the stored charge in Coulombs, and

V is the potential difference across the capacitor in units of volts.

If **a** is the inside diameter of outer cylindrical shell, **b** is the diameter of central cylinder, and **L** is the length of both cylinders, the capacitance $(\boldsymbol{C_o})$ of the cylindrical capacitor with vacuum (or free space) as the dielectric is given by:

$$\boldsymbol{C_o = \frac{2\pi\varepsilon_o L}{\ln\left(\frac{a}{b}\right)}} \tag{2}$$

where $\boldsymbol{\varepsilon_o}$ is equal to $\mathbf{8.854x10^{-12}}$ F/m and is known as permittivity of a vacuum.

Permittivity $(\boldsymbol{\varepsilon})$ relates the strength of the electrical field formed in a capacitive system to the charges on the electrodes of that capacitor (Sadiku, 2010). It is the measure of a material's resistance to the formation of an electric field. When a dielectric material is introduced between two cylinders the effective electrical field decreases due to the polarization of molecules inside the material. This neutralizes the charges on the capacitor's electrodes and thus increases its capacitance. The permittivity of a material is generally defined in relation to that of free space and is expressed as:

$$\boldsymbol{\varepsilon = \varepsilon_r \varepsilon_o} \tag{3}$$

where $\boldsymbol{\varepsilon_r}$ is called relative permittivity. Relative permittivity is the ratio of permittivity of the dielectric material to the permittivity of the free space.

$$\boldsymbol{\varepsilon_r = \frac{\varepsilon}{\varepsilon_o}} \tag{4}$$

Therefore, in the presence of a dielectric material, the capacitance of a cylindrical capacitor can be written as:

$$\boldsymbol{C = \frac{2\pi\varepsilon_r\varepsilon_o L}{\ln\left(\frac{b}{a}\right)}} \tag{5}$$

Or, $$\boldsymbol{C = \varepsilon_r C_o} \quad (6)$$

This relationship shows that introduction of a dielectric between the two cylinders increases the capacitance of a capacitor by a factor equal to its relative permittivity.

From equation 4, it can be seen that the capacitance of a cylindrical capacitor depends on the diameter and length of the two cylinders and relative permittivity of the material. If the diameter and length of the capacitor are kept constant, then the only parameter that will affect its capacitance is relative permittivity. The relative permittivity for a vacuum is 1, but for other dielectric materials, this value is larger than one and is dependent on the frequency of the applied electric field. All dielectrics (except vacuum) dissipate some energy when placed in an electrical field and their relative permittivity is given in a complex form as shown below:

$$\boldsymbol{\varepsilon_r = \varepsilon_r' - j\varepsilon_r''} \quad (7)$$

The real part of the relative permittivity ($\boldsymbol{\varepsilon_r'}$) is known as the dielectric constant and is associated with the ability of the material to store energy in the electrical field. The imaginary part ($\boldsymbol{\varepsilon_r''}$) is known as the dielectric loss factor and represents the amount of electrical energy that is lost by the material in the electrical field. The dielectric loss factor is due to the combined effect of energy losses due to the relaxation mechanisms associated with time varying electrical field and the Ohmic resistances of the material.

$$\boldsymbol{\varepsilon_r'' = \varepsilon_d'' + \frac{\sigma}{\omega \varepsilon_o}} \quad (8)$$

where $\boldsymbol{\sigma}$ is the conductivity of the medium, $\boldsymbol{\omega}$ is angular frequency of oscillating electric field, $\boldsymbol{\varepsilon_d''}$ is dielectric loss associated with relaxation and $\boldsymbol{\frac{\sigma}{\omega \varepsilon_o}}$ is conduction loss.

Relative permittivity of the dielectric in a capacitor cannot be measured directly, but it can be measured through parameters of a circuit such as impedance (***Z***) and admittance (***Y***). Impedance is defined as the total opposition of an electrical circuit or device to alternating current (AC) at a given frequency. It is a complex quantity (***R*+ *jX***) in which the real part (***R***) is resistance of the circuit and the imaginary part (***X***) is reactance. Reactance can take inductive or capacitive forms. Admittance is the reciprocal of impedance where the real part (***G***) is conductance and the imaginary part (***B***) is susceptance.

$$\boldsymbol{Y = G + jB} \tag{9}$$

Conductance is associated with losses in the dielectric material and can be written as:

$$\boldsymbol{G = 2\pi f C_o \varepsilon_r^{''}} \tag{10}$$

where f is the frequency of the sinusoidal excitation signal and C_o is the capacitance of an empty capacitor with free space as the dielectric. Similarly, susceptance is the measure of polarizability and is associated with the energy storage capacity of the dielectric. For a capacitive form of the material it can be written as:

$$\boldsymbol{B_c = 2\pi f C_o \varepsilon_r'} \tag{11}$$

Since loss of energy is inherent in dielectric materials, loss tangent can be used to express the dissipative property of the capacitor. Using equations 9 and 10, the loss tangent can be written as:

$$\boldsymbol{tan\delta = \frac{G}{B_c} = \frac{\varepsilon_r^{''}}{\varepsilon_r'}} \tag{12}$$

where $\boldsymbol{\delta}$ is the angle in the impedance plane between the negative imaginary axis and the impedance magnitude vector in the counter-clockwise direction.

Accurate measurement of changes in dielectric properties can provide valuable insight into the changing behavior or characteristics of a material. There are several factors that can affect a material's dielectric properties other than frequency. They are temperature, mixture, pressure, and molecular structure of the material. The dielectric sensor developed in this research was primarily used to measure the change in dielectric properties of the fluid (hydraulic fluid or air) due to the mixing of different components with the fluid.

In the research with a hydraulic fluid, the test fluid was mixed with iron powder and ISO test dust, which is 65-78% silicon-dioxide by weight. This mixture should change the effective permittivity of the resulting mixture and can be estimated theoretically by using Maxwell Garnett's mixing rule (Sihvola, 2000). According to Maxwell Garnett's equation, the effective permittivity depends on the permittivity of the constituents, temperature and volume fraction of the particles in the host medium. Since the relative permittivity of iron and silicon dioxide are infinite and 3.9, respectively, at all temperatures, oil contaminated with these particles should have higher effective permittivity. The theory also suggests that effective permittivity of the contaminated oil should increase with increases in the volume fraction of particle contaminants.

In past research performed using iron and soot contaminants, increases in effective permittivity with increasing contamination level were observed in the lubrication oil (Zhu et al., 2013). In another research project, the relative dielectric constant of the lubricating oil was found to increase with addition of water droplets (relative permittivity of 80) and ferrous powder (Dingxin et al., 2009). The change in loss tangent has also been used to detect the contamination of lubricant oil (Pérez and Hadfield, 2011). In proof-of-concept research preceding this project, Aziz et al. (2007, 2009) were able to show good performance in

predicting water, metal, and dust contaminant levels in hydraulic fluids. All these past results support the hypothesis that measurements of dielectric properties have the potential to detect different types of contaminants and their different levels in hydraulic oil.

As mentioned before, relative permittivity is dependent on the frequency of a time-varying electric field. At multiple frequencies, different types of dielectric mechanisms occur leading to variation in dielectric constant and loss factor of the material (Figure 2). Measuring these dielectric properties at various frequencies could provide more robust information on condition of the dielectrics. This measurement technique is known as dielectric spectroscopy. This technique can be used to not only investigate pure materials of any sizes but their interactions in mixtures as well (Tuncer et al., 2002).

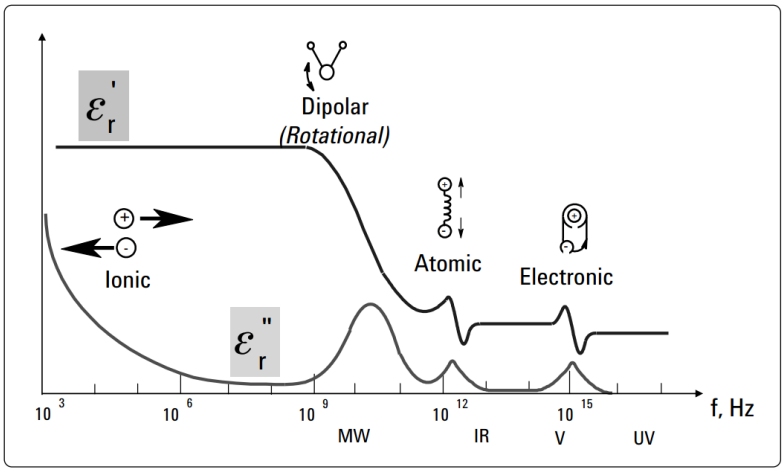

Figure 2. Frequency response of dielectric mechanisms in water (Source: Basics of Measuring the Dielectric Properties of Materials, Application note (2006))

The objective of this research was to develop a sensor that could detect different contamination levels of fluid based on dielectric spectroscopy. A short circuit and open circuit test could have been used to obtain measurements of dielectric properties at different contamination level and frequencies. However, this kind of characterization of fluid was

beyond the scope of the research and emphasis was given to the comparative investigation of fluid at different levels of impurities. Furthermore, the sensor was developed to measure contaminants in a moving fluid. Since the quantity of contaminants in the moving fluid is not constant, it is difficult to accurately predict the dielectric properties of contaminated fluid with higher certainty.

Measurement and Design

The measurement of the material under test (MUT) can be simplified with an equivalent circuit model as shown in Figure 3. The MUT is any dielectric between two electrodes of a capacitor. When an alternating current is applied to the capacitor, the resulting current will consist of a charging current (I_C) and a loss current (I_L). The charging and loss currents are associated with capacitance (C) and conductance (G) of the MUT, respectively. Any changes in amplitudes and phase of current or voltage can be used to measure the changes in the dielectric properties of the MUT.

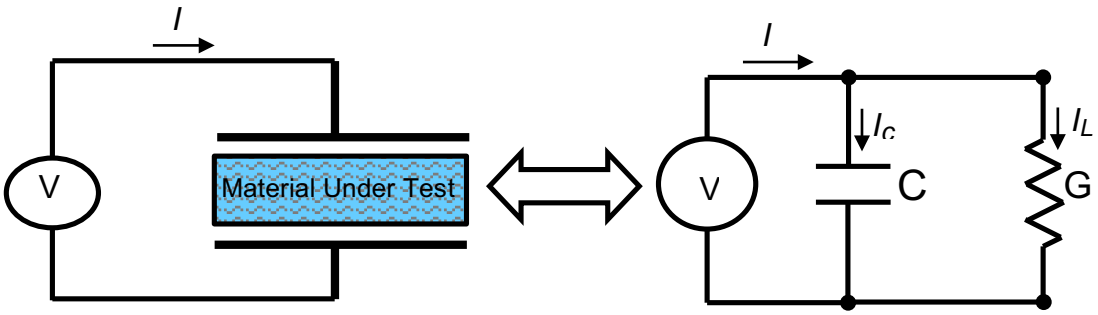

Figure 3. Physical representation (a) and equivalent circuit model (b) for material under test.

Since sensor design is vital for accurate measurement, several aspects were considered to improve performance of the dielectric sensor. One of the techniques used to minimize measurement error of the sensor was guarding or shielding. Without guarding, the

outer edge of the two electrodes of a capacitive sensor would produce a fringing electrical field which would lead to measurement errors due to the measurement of materials other than the MUT. This fringe effect can be more easily illustrated for a parallel plate capacitor (Figure 4a). Introducing guards and driving them (with another amplifier) to the same potential as the electrodes measuring the MUT can straighten the field lines at the edges and enable more accurate capacitance measurement of the MUT (Figure 4b). For the dielectric sensor, two metallic rings (or guard rings) were placed on either sides of the outer conductor.

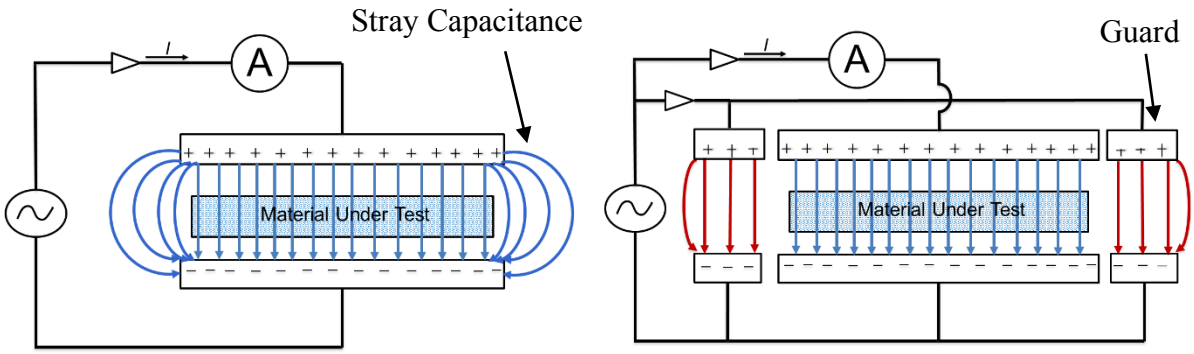

Figure 4. Electrical field lines in a parallel plate capacitor (a) without guard rings (b) with guard rings

Furthermore, electrical fields are not selective and are formed whenever there is separation of charge between two objects (Figure 5a). Shielding was employed to make the sensor more robust to the formation of electric fields with other materials external to the sensor (Figure 5b). In the case of the sensor designed for this work, shielding was accomplished with an additional metallic cylindrical shell surrounding the outer electrode. The shield was also kept at the same electrical potential as the outer electrode. In the absence of a shield, there would be coupling between the outer electrode and surrounding objects, which could result in measurement error. With the shield, stray capacitance could be substantially reduced, and the sensor could provide more accurate measurements.

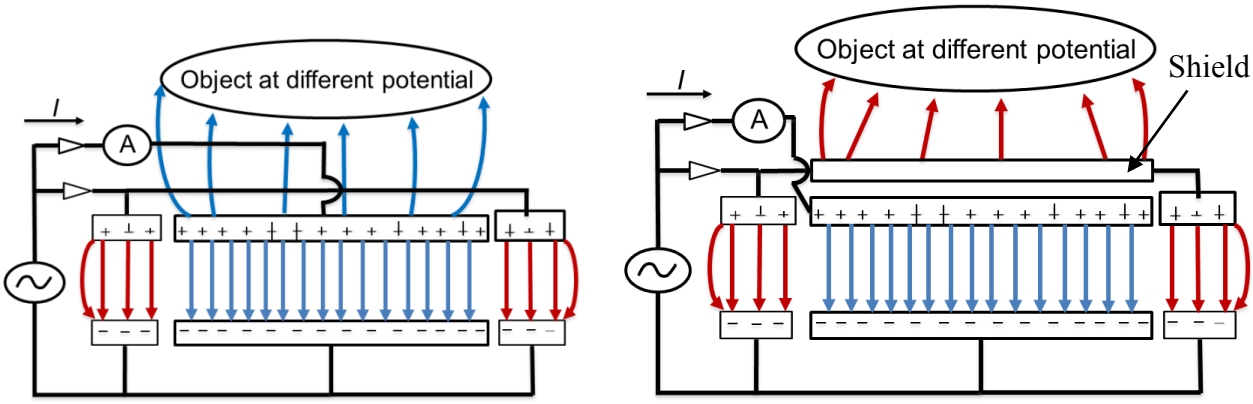

Figure 5. Electrical field lines in a parallel plate capacitor (a) without shield (b) with shield.

A number of design requirements were considered to identify the appropriate geometric sizes required for different parts of the sensor. It should be noted that these considerations were mostly developed to address design requirements for the hydraulic fluid research. They were equally applicable for research with compressed air. One of the requirements was to maintain laminar fluid flow through the sensor and to minimize dead zones where contamination particles could accumulate. To achieve this criterion, the dimensions of the inner diameters of the outer electrode and the hydraulic connector (SAE O-ring boss (ORB) male) were matched. Similarly, another requirement was matching the electrical impedance of the capacitive sensor with that of the electrical source. This requirement was based on the assumption that impedance matching was needed during high frequency operation to yield maximum power transfer between the source and the sensor and thus, to maximize sensor sensitivity. Therefore, a ratio was derived based on the principle of characteristic impedance for a coaxial line (cylindrical capacitor) shown below:

$$Z_o = \frac{60}{\sqrt{\varepsilon_r}} \ln \frac{a}{b} \tag{2}$$

The characteristic impedance, Z_o, was set equal to 50 ohms, a typical impedance for most electrical sources, and ε_r was 2.3 for hydraulic oil. Substituting these known values in equation 14, the equation was reduced to the fixed ratio of **3.44** between the diameters of the outer conductor and the central rod.

To minimize complexity in machining and pressure drop, -16 SAE ORB connectors were selected to connect the sensor to the hydraulic circuit. This choice enabled identification of the diameter required for the outer conductor (outer electrode). Subsequently, the ratio obtained from impedance matching was used to set the initial central rod (central electrode) diameter. Thus initially 6.35 mm diameter central rod was used for the test based on impedance matching. However, tests with this rod size resulted in higher error than expected probably because the low sensing capacitance of the sensor, due to the small central rod, relative to stray capacitances reduced sensitivity. Therefore, the diameter of the central rod was increased to 17.7 mm in the subsequent tests, and sensor performance improved for the larger diameter rod.

Besides the requirements mentioned above, another requirement was that the sensor produces a low-pressure drop. Equations were developed for pressure drop analysis, which showed that the pressure drop for ISO VG 46 hydraulic oil was relatively low (0.96 kilopascal or 0.14 psi) for the selected dimensions and flow rate of 350 ml/min.

Sensor design

The sensor developed in the research project can be divided into three parts: housing, tubular sensing and insulating unit, and hydraulic adapter (Figure 9). Each part is described in the sub-sections below:

Housing

The housing was fabricated from aluminum alloy 2024-T3. This alloy was chosen because of its low cost, low density, high strength, and machinability. The housing consisted of two halves that were aligned with pins and fastened together with bolts (Figure 6). This split housing design was necessary for assembly of the prototype sensing unit, but could be simplified in the future. There were circular threaded ports on either end of the housing to receive adapters for standard hydraulic couplings. The two adapters at the opposite ends of the sensor consisted of –16 SAE ORB female ports for hydraulic connections. The housing enclosed the sensing unit and was electrically grounded. The housing was designed for flexibility to accommodate sensing unit modifications and different hydraulic adapters. In fact, an alternative sensing unit was designed for this system, but was never built because the first sensing unit performed well.

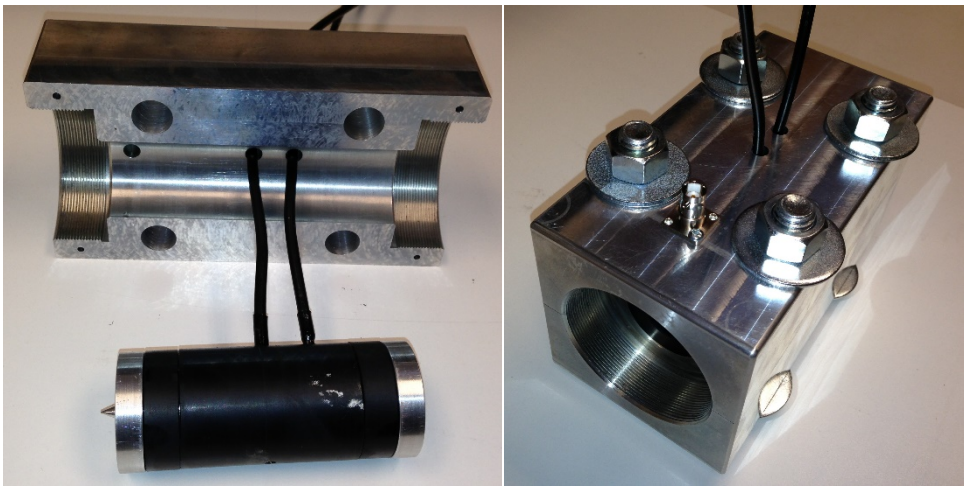

Figure 6. Sensor split housing design enables the assembly of the sensing unit and connection to cables (left) and complete assembly of the sensor (right).

Coaxial sensing and insulating unit

The coaxial sensing unit fit into the cylindrical cavity formed by the two halves of the housing (Figure 6). The unit consisted of a number of parts made up of metallic and

dielectric materials (Figure 7). These parts were designed to allow passage of oil during the measurement. This design enabled the sensor to be connected in-line within a hydraulic circuit.

The metallic parts were the central rod, outer conductor, guard rings, shield, and rod holders (Figures 8 and 9). The main sensing section was designed as a cylindrical capacitor in which the central rod and outer conductor formed the two main electrodes of the capacitive sensing unit. The hydraulic fluid between these two electrodes acted as a dielectric and had a direct relationship to the capacitance of the sensor. In this research, the goal was to capture variation in the dielectric properties of the fluids, passing through the coaxial sensing chamber, as indication of change in the contamination level of that fluid.

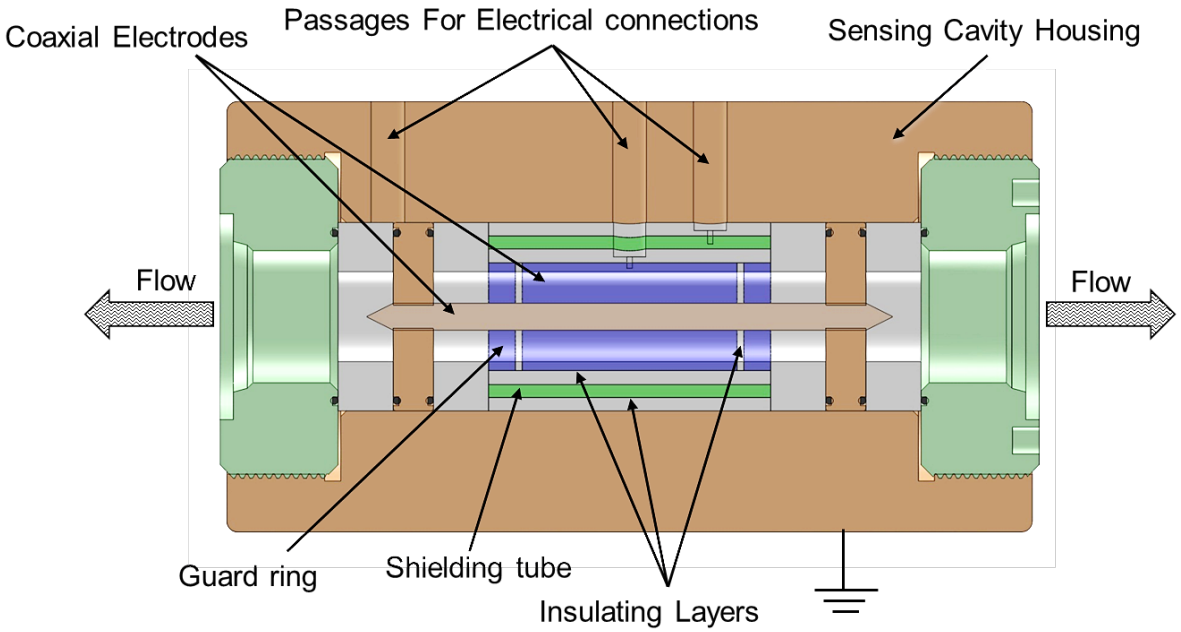

Figure 7. Cutaway view of the sensor housing shows the housing as well as the cylindrical sensing chamber. Light brown, blue and green parts are metallic while white parts are dielectrics made up of fluorinated ethylene-propylene (FEP).

Figure 8. The sensing unit's outer electric electrode assembly consisted of 12 parts made from metal and polymer materials. The sensing unit also consisted of a rod and two rod holders (not shown).

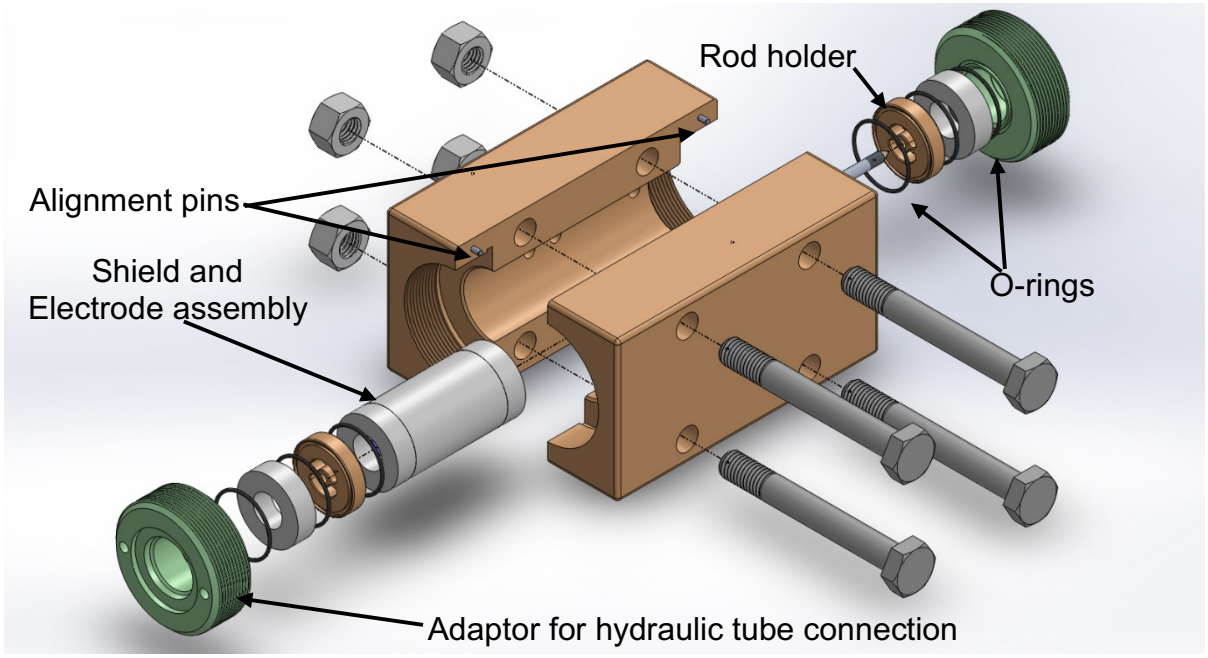

Figure 9. Exploded view of the sensor showing arrangement of different metallic and dielectric parts inside the sensor

The central rod was fabricated out of 6061 aluminum alloy. It had tapered ends to allow hydraulic fluid to pass through the sensor with minimal turbulence. It was held in place by two rod holders. The cylindrical shell surrounding the central rod is the outer conductor. It was made up of AISI type 304 stainless steel. This layer was called the outer electrode because was the larger electrode and surrounded the central rod electrode. The

outer electrode received the sinusoidal electrical signal. On either side of the outer electrode, two guard rings were placed coaxially and separated from the outer electrode by thin dielectric rings. These guard rings were also made up of 304 stainless steel. These rings were used to minimize fringe effects from edges of the outer electrode, and thus, focus the electric field on the hydraulic fluid in the sensing volume. The concentric metallic layer surrounding outer electrode and guard rings was the shield. It was made up of same material as the outer electrode and the guard rings. It also received a separate electrical signal. The shield and guard rings were connected to each other by two small metallic springs, which ensured electrical conduction was maintained between these two parts. The shield and guards were driven independently of the outer sensing electrode so that sensing area was isolated from any potential external disturbances such as electrical noise. The two circular rod holders with kidney shaped openings held the central electrode in its position. The dielectric parts in the sensing unit served as electrical insulators and physical spacers. These components were fabricated from fluorinated ethylene-propylene (FEP; PBY Plastics, Ontario, Calif.). It was selected because of its stable dielectric constant and low loss factor over a wide range of high frequencies, and compatibility with oil.

The metallic and dielectric parts between the two-rod holders were bonded to each other using a silicone sealant (Ultra Black, Permatex, IL), so that the oil would not leak through the adjoining surfaces. In addition, o-rings were placed on sides of the rod holders and hydraulic adapters to minimize leakage.

Summary

The dielectric properties of a material provide information on how the material will behave to an applied electromagnetic field. These properties are uniquely characteristic to the

material, and thus knowledge of them could be valuable for different applications. The dielectric spectroscopic sensor developed in the research project capitalizes on this utility for detecting typical contaminants in a hydraulic fluid and in compressed air. The dielectric sensor based on the capacitive sensing technique enables measurement of impedance and admittance at multiple frequencies. The information from these measured variables was used estimate changes in fluid contamination levels. Since there are several factors that can affect sensor performance and functionality, a number of design requirements were identified and applied to design the sensor.

REFERENCES

Agilent-Technologies, 2014. Basics of Measuring the Dielectric Properties of Materials. Application note. Retrieved July 23, 2015, from cp.literature.agilent.com/litweb/pdf/5989-2589EN.pdf

Agilent-Technologies, 2013. Agilent Impedance Measurement Handbook - A guide to measurement technology and techniques - 4th edition. Retrieved July 23, 2015, from cp.literature.agilent.com/litweb/pdf/5950-3000.pdf

Aziz, S. A., B. L. Steward, and S. J. Birrell. 2007. Dielectric spectroscopy of hydraulic fluid for contamination detection. In Proceedings of ISFP'2007: 5th International Symposium on Fluid Power Transmission and Control, Beidaihe, China, June 6-8.

Aziz, S. A., B. L. Steward, S. J. Birrell. 2009. Multifrequency dielectric sensing for hydraulic fluid contamination detection. NFPA Fall Conference, Wheeling, IL.

Carey, A. A., and Hayzen, A. J. 2001. The Dielectric Constant and Oil Analysis. Retrieved May 16, 2014, from http://www.machinerylubrication.com/Read/226/dielectric-constant-oil-analysis

Dingxin, Y., Xiaofei, Z., Zheng, H., and Yongmin, Y. 2009. Oil Contamination Monitoring Based on Dielectric Constant Measurement. In International Conference on Measuring Technology and Mechatronics Automation, 2009. ICMTMA '09 (Vol. 1, pp. 249–252).

Johnson L., G. 2001. Chapter 3 - Lossy Capacitors. In Solid State Tesla Coil. Manhattan, KS.

Sadiku, M. 2010. Elements of Electromagnetics (5th ed.). New York: Oxford University Press.

Pérez, A. T., and Hadfield, M. 2011. Low-Cost Oil Quality Sensor Based on Changes in Complex Permittivity. Sensors (Basel, Switzerland), 11(11), 10675–10690.

Sihvola, A. 2000. Mixing Rules with Complex Dielectric Coefficients. Subsurface Sensing Technologies and Applications, 1(4), 393–415.

Tuncer, E., Serdyuk, Y. V., and Gubanski, S. M. 2002. Dielectric mixtures: electrical properties and modeling. IEEE Transactions on Dielectrics and Electrical Insulation, 9(5), 809–828.

Zhu, J., Yoon, J., He, D., Qiu, B., and Bechhoefer, E. 2013. Online condition monitoring and remaining useful life prediction of particle contaminated lubrication oil. In 2013 IEEE Conference on Prognostics and Health Management (PHM) (pp. 1–14).

CHAPTER 3: DIELECTRIC SPECTROSCOPIC SENSOR FOR PARTICLE CONTAMINANT DETECTION IN HYDRAULIC FLUIDS

A paper to be submitted to the *International Journal of Fluid Power*

Safal Kshetri, Brian L. Steward, and Stuart J. Birrell

Abstract

Particulate contamination of hydraulic fluids is one of the major causes of mechanical wear of hydraulic components resulting in system inefficiency and failure. Potential failures of hydraulic systems could be avoided by continuously monitoring of fluid condition. A practical contaminant sensor was developed to estimate the level of particle contamination in hydraulic fluids. The sensor was designed to be installed on off-highway vehicles and provide in-line estimates of contaminated hydraulic fluid cleanliness. The sensor used dielectric spectroscopy for measuring contaminants. To investigate the performance of the dielectric sensor, tests were performed using iron powder and ISO test dust (ISO 12103-1, A3 medium) as hydraulic contaminants. A hydraulic test circuit was built, and a methodology was developed for the tests. An eight-channel particle counter was used for calibration of the dielectric sensor. PLS models were developed to investigate the relationship between dielectric spectra and contaminant particle counts. The RMSEC and RMSECV for the sensor with a central rod diameter of 6.35 mm (0.25 in.) were 1.1 and 1.39 of adjusted ISO fluid cleanliness codes, respectively, for iron powder. For a 17.7 mm (0.70 in.) diameter central rod, the respective RMSEC and RMSECV values were 0.62 and 0.83 for iron powder and 1.29 and 1.48 for ISO test dust. The sensor shows good potential for estimating the cleanliness level of hydraulic fluid in the context of particle contaminants.

Keywords. dielectric sensor, dielectric spectroscopy, ISO 4406 fluid cleanliness code, particle contaminants

Introduction

Advances in fluid power system technology have led to the development of sophisticated high-pressure systems. These systems need high quality and clean fluid for reliable and efficient operation. About 70 percent of all hydraulic system failures are due to contaminants in the fluid (Singh et al., 2012). Even if a failure does not occur immediately, the high levels of contamination can reduce hydraulic system efficiency. Increasing contamination levels and changes in the fluid properties could be clues of impending hydraulic component failures. A sensor capable of continuously monitoring fluid condition during equipment operation could have significant impact by preventing machinery failures with associated losses.

Hydraulic fluid condition can be determined by measuring viscosity, refractive index, density, base number (BN), acid number (AN), water content, metals (additive and wear metals), color and flash point. Changes in fluid dielectric properties are another indication of changes in the quality of the working fluid (Carey and Hayzen, 2001). The oxidation and depletion of additives will affect fluid chemistry. Additionally, the presence of contaminants such as water, soot particles, acid combustion particles, glycols, ferrous and non-ferrous metallic particles could also lead to changes in dielectric properties (Perez and Hadfield, 2011).

Particle counting is the most common method used for detection of contaminants in a hydraulic fluid. Commercially available automatic particle counters sense light blockage by particles and use the ISO fluid cleanliness code (ISO 4406:1999) to report the level of solid particle contamination of the fluid. The ISO 4406:1999 standard provides a standard means for reporting of particle count data by converting the numbers of particles into broad classes

or codes based on particle size. The reported code is expressed in a three number format; for example, 22/18/13, where the first, second and third scale numbers separated by slashes represent a logarithmic scale related to the number of particles equal to or larger than 4μm, 6 μm, and 14 μm, respectively, in one milliliter of fluid (ISO 4406:1999). The volume of particles in a fluid influences its dielectric properties. Therefore, a sensor capable of measuring dielectric properties could be calibrated to automatic particle counters and estimate fluid contamination level in a lower cost and more robust manner for mobile applications.

The dielectric properties of a material explain the electrical interaction between the material and an electric field. Normally, this interaction depends on the frequency of the applied field and can be described best using relative complex permittivity, $\varepsilon_r = \varepsilon_r' - j\varepsilon_r''$, where the real part ε_r' denotes the dielectric constant of the material and the imaginary part ε_r'' denotes the dielectric loss factor. The dielectric constant is a measure of the ability of the material to store electrical energy; while the loss factor is a measure of energy loss in a material relative to the applied external electrical field. The relative complex permittivity can be measured as a function of frequency using dielectric spectroscopy (Von Hippel). Dielectric spectroscopy has been used for comparing different petroleum fractions (Folgero; Tjomsland, Hilland and Christy), sensing moisture dynamics in oil impregnated pressboard (Sheiretov and Zahn, 1995), and monitoring of moisture content and insulation degradation in oil transformers (Koch and Feser, 2004).

The objective of this research was to investigate the ability of a sensor to estimate the level of iron particle contaminants and ISO test dust using dielectric measurements of hydraulic fluid passing through the sensor. The sensor was designed to be low cost for off-

road vehicle installation and to provide in-line measurements of contaminants during operation.

Materials and Methods

Dielectric properties of the hydraulic test fluid samples were measured using an impedance analyzer (model 4192 LF, Hewlett-Packard, Palo Alto, CA, USA) connected to the dielectric sensor developed in the research project. Conductance and susceptance, which contain dielectric information of the material under test, were measured over frequencies ranging from 5 Hz to 13 MHz. An experimental hydraulic apparatus was developed for testing dielectric sensor performance. Finally, the partial least squares (PLS) regression method was used for analysis of the experimentally collected data.

Dielectric Sensor Design

The dielectric sensor designed and fabricated for testing consisted of three parts: the housing, the sensing unit, and the hydraulic adapter. The housing (Figure 10) was built to primarily enclose and support the sensing unit and to provide connections for the hydraulic adapters. The split design of the housing was necessary for simplifying electrical connections to the sensing unit. The dimensions of the tubular passage and threaded ports of the housing were chosen to provide flexibility in accommodating any future modifications of sensing unit and hydraulic adapters. The housing also has an electrical connector for grounding the case during measurements.

The sensing unit (shield and electrode assembly) was designed to fit into the tubular passage formed by the two halves of the housing. The unit was built by assembling a number of metallic and dielectric parts that were fabricated to allow passage of fluid through the sensor (Figure 11). This design enabled the sensor to be connected in-line with a hydraulic

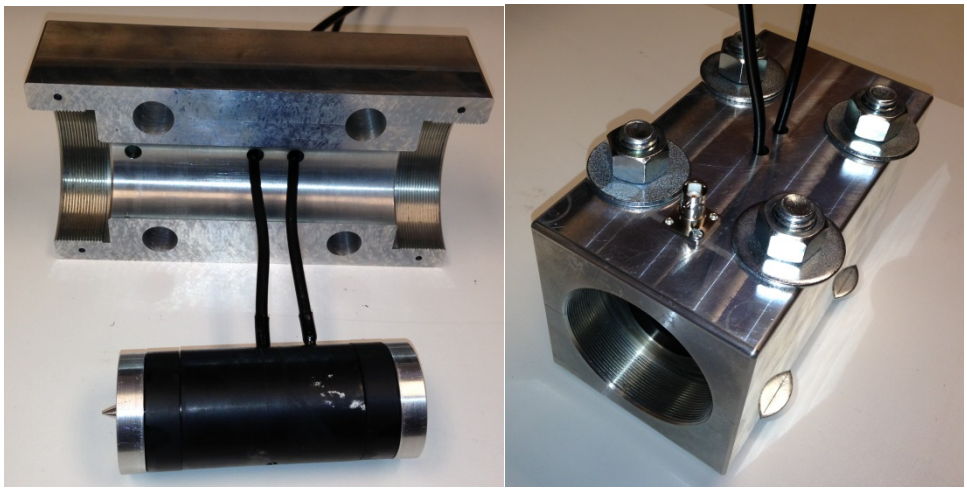

Figure 10. Sensor split housing design enables the assembly of the sensing unit and connection to cables (left) and complete assembly of the sensor (right).

circuit. The metallic parts of the sensing unit are the outer conductor, central rod, guard rings, shield, and rod holders (Figure 12). The main sensing section of the unit was designed as a cylindrical capacitor in which the outer conductor and central rod form the two main electrodes of the capacitive sensing unit. The outer conductor was connected to a short coaxial cable for receiving electrical input signals, while the central rod, lying inner and coaxial to the outer conductor, was electrically grounded through metallic rod holders that make physical contact with the housing. The rod holders with kidney shaped openings were machined to hold the central conductor in its position. Any medium between the two coaxial electrodes acts as a dielectric and has direct influence on the capacitance of the sensor.

The diameter of the outer conductor was chosen to match with that of the hydraulic connector to promote laminar fluid flow. A nominal 1-inch internal diameter (-16) SAE O-Ring Boss hydraulic connection was selected to ease manufacturability and minimize pressure drop. The central rod was designed with gradually tapering ends to maintain steady fluid flow through the sensing unit.

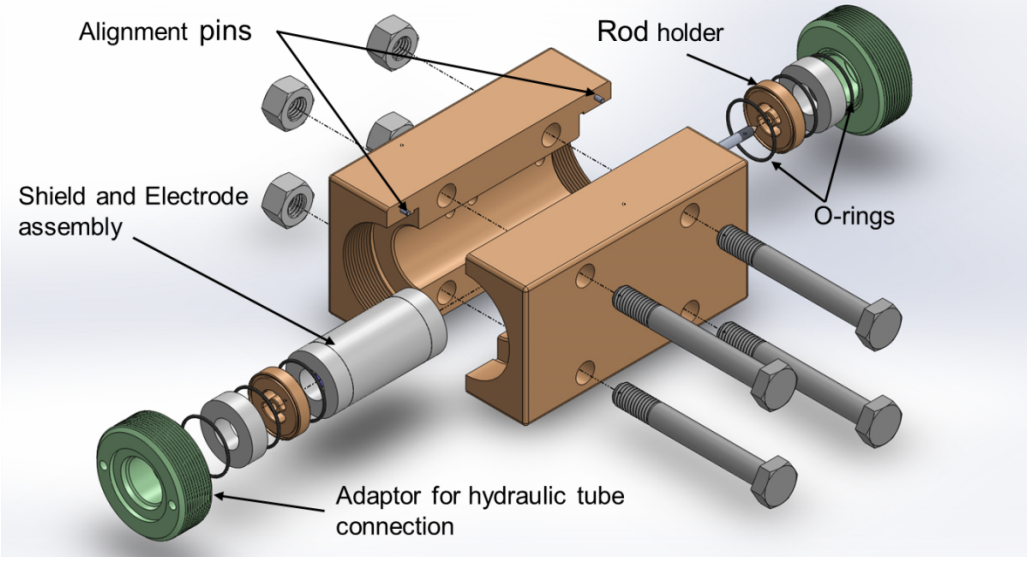

Figure 11. Exploded view showing flow-through design of the sensor and arrangement of different metallic parts and dielectric assembled

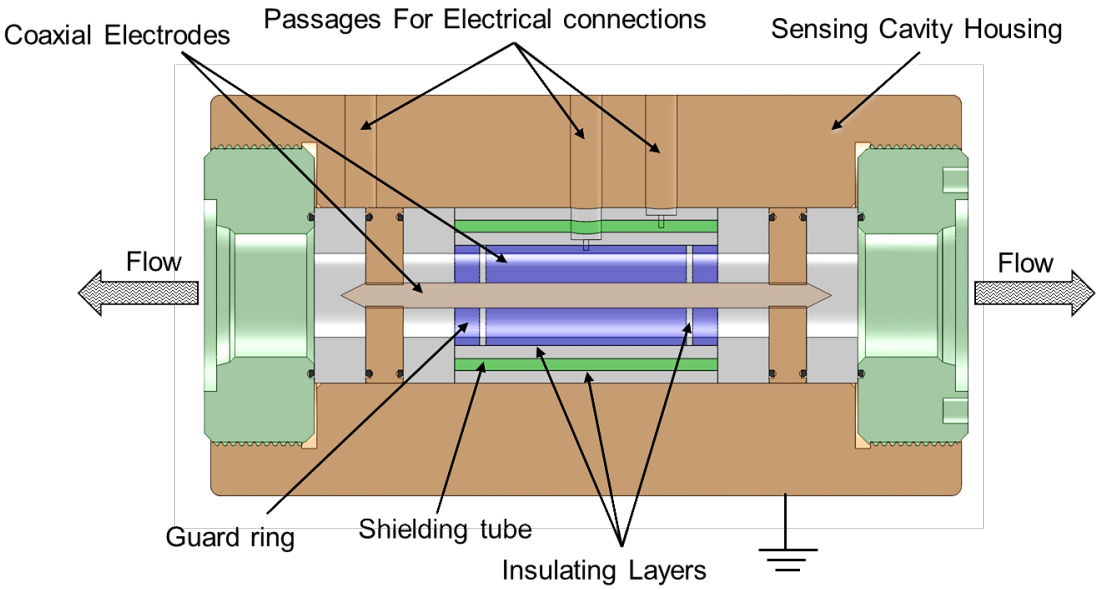

Figure 12. Cutaway view of the sensor housing shows the housing as well as the coaxial sensing unit with different metallic and dielectric parts.

On either side of the outer conductor, two metallic guard rings were placed coaxially and separated from the outer conductor by thin dielectric rings. These rings were used to minimize fringe effects from the edges of the outer conductor, and thus, focus the electric flux on the fluid in the sensing volume. The outer conductor and guard rings were surrounded

by a tubular metallic layer called a shield. The shield and guard rings were connected to each other by two small metallic springs, which ensured electrical conduction was maintained between these two parts. A short coaxial cable was attached to the shield to maintain it at the same voltage as the outer conductor. The shield and guards were driven independently of the outer conductor, so that the sensing area was isolated from any potential external electrical disturbances.

The dielectric parts in the sensing unit were used as electrical insulators and physical spacers. These components were fabricated from fluorinated ethylene-propylene (FEP). FEP was chosen as a dielectric material for its stable dielectric constant and low loss factor over a wide range of low to high frequencies, and compatibility with oil. Hydraulic adapters were machined to fit into the threaded portion of the housing. These adapters had -16 SAE O Ring Boss female ports for connection to a hydraulic circuit.

Hydraulic test circuits

The hydraulic circuits developed to test the dielectric sensor consisted of a fluid cleaning circuit and a test circuit (Figure 13). In general, the hydraulic fluid in an oil drum comes from the manufacturer with particle contaminants. Therefore, the fluid cleaning circuit (Figure 13a) was used to clean the hydraulic fluid before it was introduced into the test circuit (13b). The fluid cleaning circuit consisted of two filters (model Ultipleat® UE219AN08H, Pall Corp, Port Washington, NY and model SP15/25 P/N P564967, Donaldson, Bloomington, Minn.) through which the hydraulic fluid was circulated several times and then transferred to the test circuit. The test circuit consisted of two reservoirs. One of them stored contaminated fluid prepared in the laboratory by mixing a high dose of iron particles with the clean fluid, while the other was used to store clean fluid used for testing.

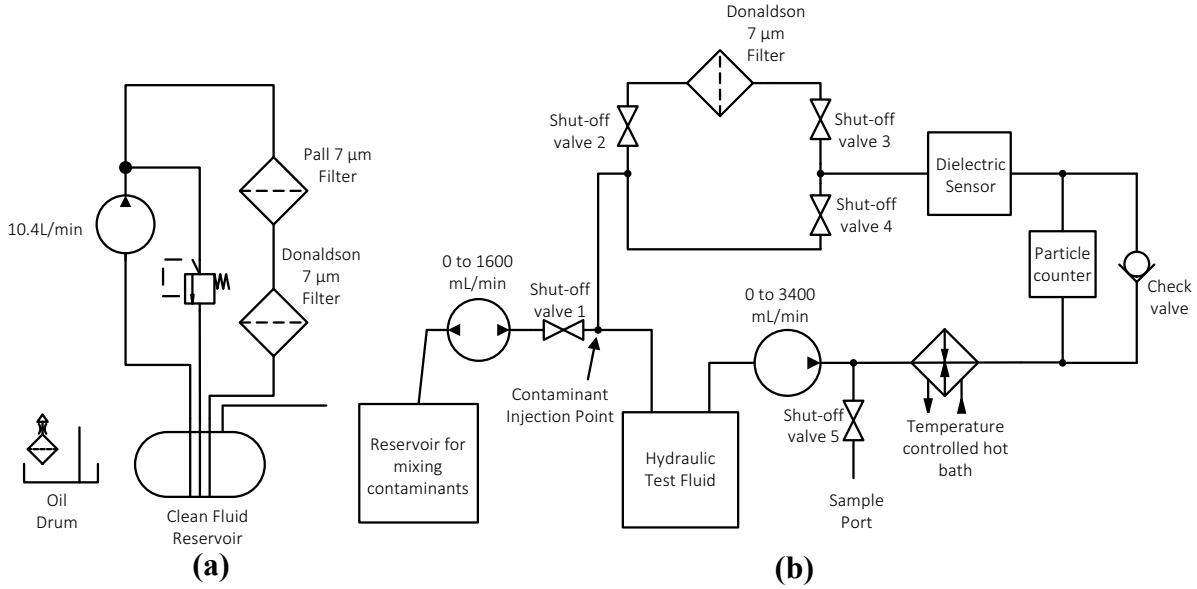

Figure 13. The test circuits consisted of (a) fluid cleaning circuit and (b) the sensor test circuit.

Peristaltic pumps were used to move the fluid in the circuit while minimizing the introduction of additional particles due to internal wear. A filter was added in the test circuit to ensure the test fluid achieved the desired ISO cleanliness level required at the beginning of the experiment. The fluid passed through a coil in a constant temperature bath to maintain steady fluid temperature throughout the experiment. To calibrate the dielectric sensor, an in-line, light-blockage particle counter (model ICM, Mpfiltri, Quakertown, PA) was added in the test circuit. Shut off valves and check valves were used to achieve desired flow operation required during the experiment.

Test procedure

Three tests were performed with solid particulates as hydraulic contaminants. The initial two tests were performed with iron powder using the central rods of different diameters. The first test was performed using the rod diameter of 0.25 inch (6.35 mm). This diameter was initially considered in the research for impedance matching of the dielectric

sensor with electrical source to maximize electrical power transfer. However, after realizing that this rod size led to a small sensing capacitance relative to stray capacitance, a second test was performed with a larger rod diameter of 0.70 inch (17.7 mm) to determine if it would improve the sensing performance. The third test was performed with ISO test dust using the larger rod diameter.

The iron powder (CAS: 7439-89-6; P/N 00170, Alfa Aesar, Ward Hill, MA) used in the test consisted of spherical iron particulates less than 10 μm in diameter. The ISO medium test dust (ISO 12103-1, A3 medium, Powder Technology Inc., Burnsville, Minn.) had mixtures of chemical particulates (SiO_2, Al_2O_3, Fe_2O_3, Na_2O, CaO, MgO, TiO_2, K_2O) less than 176 μm in diameter. The hydraulic fluid used during the test was an ISO VG 46 hydraulic oil (Tellus, Shell, Houston, TX). Prior to each test, the hydraulic fluid was cleaned in the fluid cleaning circuit. About 1000 ml of this clean fluid was drawn out into a reservoir and mixed with test particulates to produce a highly concentrated contaminant fluid mixture. In the test circuit reservoir, 2000 ml of clean hydraulic fluid was stored as the test fluid. This fluid was continuously stirred using magnetic stirrer to minimize settling of the particulate contaminants. The temperature controlled hot bath maintained a steady fluid temperature of approximately 34 degrees Celsius throughout the tests. The electrical terminals of the dielectric sensor were connected to the impedance analyzer.

The test fluid was circulated through the test circuit, and the ISO cleanliness level was monitored using the particle counter. Filtration was used to bring the ISO cleanliness level to the desired base level. The experiment was started after temperature and cleanliness level reached a steady state. Clean fluid at the base level was the first sample measured using the impedance analyzer. A small amount of the contaminant mixture fluid was then injected

to the test fluid in a controlled manner to produce a sample test fluid with the ISO cleanliness code level slightly higher than before. After the ISO cleanliness level reached steady state, dielectric measurements were acquired for this new sample test fluid. This process of injecting contaminants and taking measurements was continued until the test fluid reached the highest level of contamination that the particle counter could effectively measure. This experiment was replicated three times. To make the replications independent, after completion of each replication, the test circuit was flushed out with clean fluid and a new volume of test fluid was used for next replication.

To acquire measurements from the dielectric sensor, the impedance analyzer was programmed to measure both conductance and susceptance at 63 frequencies ranging from 5 Hz to 13 MHz sampled linearly within decades. These dielectric spectroscopic measurements were acquired three times for each sample. At the same time, particle count measurements were acquired over 60 second time intervals, usually resulting in acquisition of nine particle count samples while the dielectric measurements were being acquired.

Data Analysis

After the completion of the tests, partial least squares regression (PLS regression) analysis was performed to develop models relating spectral measurements to particle counts from the particle counter. The ISO 4406:1999 cleanliness code from the particle counter was not directly correlated with the spectral data. The dielectric sensor was measuring bulk dielectric properties of the fluid, as a result larger individual particles would have greater influence on dielectric response of the sensor because of their ability to displace a larger fluid volume than the smaller particles in the fluid. Therefore, a weighted composite cleanliness code was developed using the data from the particle counter. To develop this weighted code,

ranges of particle sizes were selected to form equivalent ISO code ranges (Table 1) using particle sizes reading from the eight measurement channels of the particle counter (>4, 6, 14, 21, 25, 38, 50, 68 μm(c)). The volume of the mean-sized particles in the range was calculated and a relative multiplier was developed using 5 μm as reference particle size (Equation 14). This multiplier gave the number of 5 μm particles that would be needed to produce a volume equivalent to the particle volume of a particle in a different ISO code range.

Table 1. ISO code range and parameters used for developing adjusted ISO cleanliness code

ISO code range (i)	Mean Diameter in Range, $\boldsymbol{X}$ (μm)	Volume V_X (μm)^3	Relative Multiplier $V_{X_{i\_wrt\_5\mu m}}$
4 - 6	5	65	1
6 - 14	10	524	8
14 - 21	17.5	2806	43
21 - 25	23	6371	97
25 - 38	31.5	16365	250
38 - 50	44	44602	681
50 - 68	59	107539	1643

If X_i denotes any mean diameter in the ISO code range, then the relative multiplier, $V_{Xi\_wrt\_5\mu m}$, for particular volume of mean diameter particle (V_{X_i}) can be written as:

$$V_{X_{i\_wrt\_5\mu m}} = \frac{V_{X_i}}{V_{5\mu m}} \tag{34}$$

and, if (n1, n2,…, n7) denote particle counts for the corresponding ISO code ranges, the volume weighted count, V_{wc}, can be written as:

$$V_{wc} = \sum_{i=1}^{7} n_i V_{X_{i\_wrt\_5\mu m}} \tag{15}$$

This calculation generated a value that was approximately equal to number of 5 μm particles needed to make up the total particle volume detected by the particle counter.

For PLS analysis, particle counts corresponding to ISO code range (>4-6) was used for regression with spectral data. Since the count for this range from particle counter does not represent the actual volume of particles flowing through the sensor, a ratio was developed representing the contribution of the count in this range to the volume weighted count. The ratio for any sample in a test, R_m, is given as below:

$$R_m = \frac{n1}{V_{wc}} \tag{16}$$

where n1 represent the count for particle sizes 4 to 6 μm from the particle counter in 100 ml of a sample

Since the contribution of the count at this range differed for different samples (contamination level reading) in the test, an average of the ratio was calculated from all the samples in the test (Equation 17), and the adjusted volume weighted count, V_{adj_count} for each sample was calculated by multiplying the mean ratio with its volume-weighted count (Equation 18).

$$\boldsymbol{R_{avg}} = \frac{\sum_{m=1}^{n_m} \boldsymbol{R_m}}{\boldsymbol{n_m}} \tag{17}$$

where $\boldsymbol{n_m}$ represent the total samples in all three replications for a test

$$\boldsymbol{V_{adj\_count}} = \boldsymbol{R_{avg} V_{wc}} \tag{18}$$

ISO code models are developed based on the base-two logarithmic relationship between the ISO codes and the particle counts represented in the equation. Therefore, the adjusted ISO code, C_{adj_ISO}, developed for the analysis can be written as:

$$\boldsymbol{C_{adj\_ISO} = \log_2\left(V_{adj\_count}\right)} \tag{19}$$

Cross validation was performed to assess the predictive ability of the models. Root mean standard error of calibration (RMSEC) and root mean standard error of cross validation (RMSECV) values obtained from PLS analysis were used to analyze the performance of the dielectric sensor. RMSEC is a measure of variability in the readings of the particle counter that is not explained by the model developed using calibrated data sets, while RMSECV is an indication of the predictive performance of the sensor, in the absence of an independent data set.

Results and Discussion

The calibrated and cross-validated models obtained using PLS (Figure 14 and 15) showed that the dielectric sensor was able to capture increases in the levels of iron particulates and ISO test dust in the hydraulic fluid. There was less variation in the data for the test with the 17.7 mm diameter central rod as seen in Figure 14(a), while the data were observed to be more spread for the test with the 6.35 mm central rod using iron powder (Figure 14b) and the 17.7 mm diameter rod with ISO test dust particles (Figure 15). It shows the dielectric sensor was more sensitive in measuring iron powder in the hydraulic fluid when 17.7 mm diameter central rod was used.

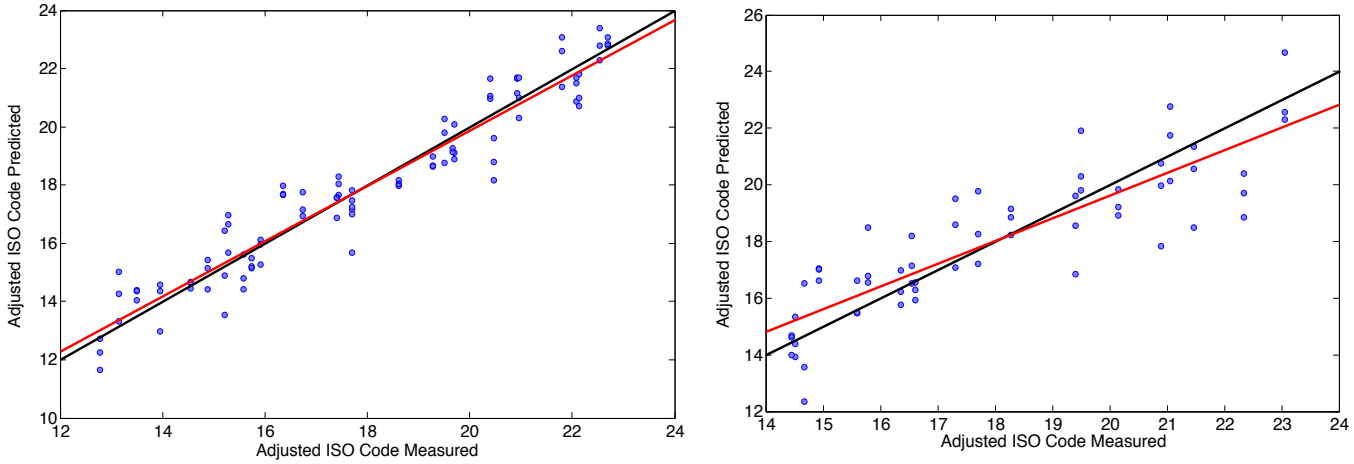

Figure 14. Predicted adjusted ISO Code against measured adjusted ISO code for the PLS cross-validation models developed using central rods of diameter (a) 17.7 mm and (b) 6.35 mm using iron powder as test contaminants. The black line represents 1 to 1 line and red line represents regression line for cross-validated model.

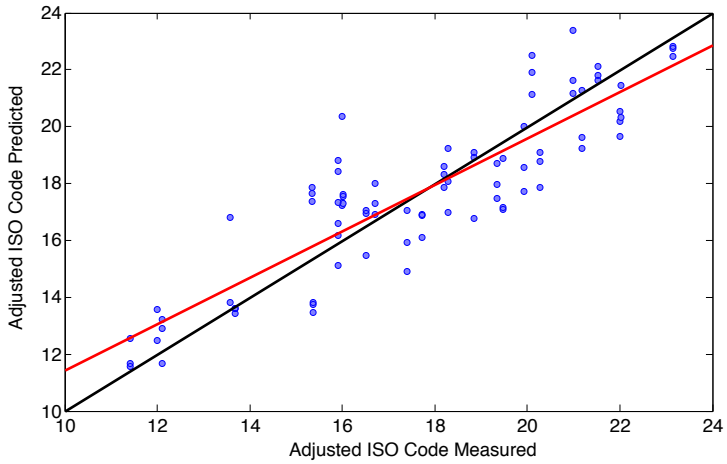

Figure 15. Predicted adjusted ISO Code vs measured adjusted ISO code for the ISO test dust PLS model. The black line represents the 1 to 1 line and red line represents regression line for cross-validated model.

The models in the PLS regression were selected based on the number of latent variables that minimized the RMSECV value. The use of additional latent values could have resulted in a model that would overfit the data. The test results obtained from three tests are based on the selection of different latent variables that can be seen in Table 2. For the test

performed with central rod of 17.7 mm in diameter and iron powder as contaminants, the RMSEC and RMSECV values were observed to be 0.62 and 0.83 respectively based on 16 latent variables. This shows that the calibration model obtained using larger rod was able to detect iron contaminants within ± 0.62 of the adjusted ISO code level, while for cross validation the result was found to be within ± 0.83 of the adjusted ISO code.

Table 2. PLS calibration and cross-validation results for two central rods

Particulate Contaminants	Central rod diameter (mm)	Number of latent variables	RMSEC (Adjusted ISO code)	RMSECV (Adjusted ISO code)	R^2
Iron Powder	6.35	9	1.1	1.39	0.7
Iron Powder	17.7	16	0.62	0.83	0.923
ISO Test Dust	17.7	9	1.29	1.48	0.78

Similarly, RMSEC and RMSECV values for 6.35 mm central rod were 1.1 and 1.39 for the test with iron powder after selecting nine latent variables. The results for the smaller rod were not as good as the ones obtained for the larger rod, as the prediction results for the calibration and cross-validation were found to be greater than 1 adjusted ISO code level. These results show that the dielectric sensor had better accuracy in measuring contaminants with larger diameter central rod. These are possible reasons for this improved accuracy. First, with larger rod diameter, the capacitance of the sensor increases, and measurements are less affected by stray capacitances. Second, the electrical field strength is almost uniform near both outer conductor and central rod when larger diameter central rod is used. As a result, particles moving close to any of these electrodes will have an equal effect on the dielectric measurement. On contrary, with a smaller diameter rod, electric field strength will be lower near one of the electrodes, and thus the sensor is less responsive when the particles

move close this electrode with lower electric field strength. This effect may result in the lower variation in the measurement observed for the larger diameter central rod as compared to smaller rod.

The RMSEC was 1.29 and RMSECV was 1.48 for the test with ISO test dust conducted using 17.7 mm diameter central rod. The calibration model detected ISO test dust particles within $\pm$ 1.29 of adjusted ISO code level, and the prediction based on cross-validation was $\pm$ 1.48. Based on these results, it can be inferred that the dielectric sensor was more sensitive to iron powder in the hydraulic fluid than ISO test dust particles. This effect was probably because the effective dielectric constant of the hydraulic fluid increased due to the very high dielectric constant of iron powder (almost infinite). On the contrary, ISO test dust consists of particulates with dielectric constant similar to that of a hydraulic fluid. For example, dielectric constant of silica (SiO_2), the major component of ISO test dust (68-76 % of weight), is around 3.9, which is closer to the dielectric constant of typical hydraulic oil (2.1 to 2.4). Probably due to this similarity, the sensor was less responsive to the presence of the test dust contaminants.

To develop PLS models for all three tests, nine or more latent variables were required mostly in order to capture variations in the particle count. These models also excluded the data associated with very low contamination of hydraulic fluids (Low ISO code level) because substantial fluctuation was observed in particle counts at this level. It should be noted that the sensor was not measuring contaminants in a static sample but varying level of contaminants in flowing fluid. Despite this nature of the measurements, it was able to capture the variation in the contamination level as verified by the results from PLS analysis.

Conclusions

From this research, the following conclusions can be drawn:

1. The results show that dielectric spectroscopy has good potential to detect different levels of contaminants, that are consistent with modern hydraulic components in a moving hydraulic fluid.
2. Dielectric spectroscopy can also be used to predict levels of completely different types of particles i.e. metals and dust in the hydraulic fluids using prediction models developed for these particles.
3. The results show that the dielectric sensor was able to detect very low level of contaminants, which should be typically avoided for use with modern hydraulic components, with reasonable accuracy.
4. The dielectric sensor has the potential to be used for identifying low and high contamination of the hydraulic with solid particles.

Acknowledgements

This project was supported by the National Fluid Power Association (NFPA) and the Iowa State Experiment Station.

REFERENCES

Carey, A. A., and Hayzen, A. J. 2001. The Dielectric Constant and Oil Analysis. Retrieved May 16, 2014, from http://www.machinerylubrication.com/Read/226/dielectric-constant-oil-analysis

Folgero, K. 1998. Broad-Band Dielectric Spectroscopy of Low Permittivity Fluids using One Measurements Cell. Instrumentation and Measurement, IEEE Transactions on, 47(4), 881-885.

Koch, M., and Feser, K. 2004. Retrieved 05 18, 2014, from www.uni-stuttgart.de: http://www.uni-stuttgart.de/ieh/forschung/veroeffentlichungen/2004_aptadm_koch.pdf

Perez, A. T., and Hadfield, M. 2011. Low-Cost Oil Quality Sensor Based on Changes in Complex Permittivity. Sensors, 11(11), 10675-10690.

Sheiretov, Y., and Zahn, M. 1995. Dielectrometry Measurements of Moisture Dynamics in Oil-impregnated Pressboard. IEEE Transactions on Dielectrics and Electrical Insulation, 2, 329-351.

Singh, M., Lathkar, G. S., and Basu, S. K. 2012. Failure Prevention of Hydraulic System Based on Oil Contamination. Journal of The Institution of Engineers (India): Series C, 93(3), 269-274.

Tjomsland, T., Hilland, J., Christy, A. A., Sjoblom, J., Riis, M., Friis, T., and Folgero, K. 1996. Comparison of Infrared and Impedance Spectra of Petroleum Fractions. Fuel, 75(3), 322-332.

Von Hippel, A. R. 1954a. Dielectric Materials and Applications. New York: The Technology Press of M.I.T and John Wiley & Sons.

CHAPTER 4. DIELECTRIC SPECTROSCOPIC CONTAMINATION SENSING IN A COMPRESSED AIR STREAM

A paper submitted to the *International Journal of Fluid Power*

Safal Kshetri, Brian L. Steward, and Stuart J. Birrell

Abstract

Contamination of compressed air can reduce its utility and lead to costly failure of pneumatic components. Monitoring the presence of contaminants in the air could provide early warning to take measures that could retain pneumatic system usefulness. The sensing of contaminants in a compressed air stream using dielectric spectroscopy has good potential for a viable commercial sensor for pneumatic systems based on the differences in dielectric properties between air and common contaminants such as metal, silicon, and water condensate. Oil mist, while not a contaminant, is required for lubricating pneumatic components, so its presence is important. Two tests were performed using a dielectric sensor capable of spectroscopic measurement to investigate the efficacy of dielectric spectroscopy in detecting the presence of liquids (water and oil) in compressed air. The first test used deionized water, and the second test used a light lubricant oil (Sunoco Sunvis 932, Sunoco, PA). Industrial spray nozzles were used to atomize these liquids, which were then entrained in a compressed airstream and passed through the dielectric sensor. Spectroscopic measurements were taken and multivariate classifiers using PCA and LDA were developed to investigate the sensor's performance in differentiating the presence and absence of liquid droplets in compressed airstream. The classifier was able to separate the two cases based on the spectroscopic data, which suggests dielectric spectroscopy could be used to detect these two liquids in the compressed airstream.

Keywords. dielectric sensor, dielectric constant, dielectric spectroscopy, PCA, LDA

Introduction

Compressed air has multiple applications owing to its useful properties. It has been used for power transmission and motion control in pneumatic systems, as well as inclusion into different processes like food packaging and processing. Because of its widespread use, it is also known as the fourth utility after water, electricity and natural gas (NREL, 2003). Unlike these other utilities, it can be generated onsite, and thus users have more control over its usage and quality.

However, inefficiency in compressed air systems can greatly reduce its utility. Low efficiency will not only lead to decreases in its productivity, but also make it a very expensive entity. According to the survey from U.S. Department of Energy, about 10% to 30% of the electricity consumed in many facilities is used for compressed air generation. Electricity costs constitute 76% of the cost of compressed air while the remaining costs are due to maintenance and equipment. Research shows that it is the most expensive form of energy available in the plant, since the conversion efficiency from electrical to pneumatic energy is as low as 10% to 19 % (Shanghai and McKane, 2008).

Technology that improves compressed air systems could have a significant impact. A study has shown that improvement in compressed air systems can reduce electricity consumption by 20% to 50 % or more, and thus save substantial expenses for energy (Saidur et al., 2010). Furthermore, a properly managed compressed air system can reduce maintenance and downtime costs, increase productivity, and improve product quality.

Contamination of compressed air is one of the prime reasons for inefficient systems. Water is a typical contaminant found in compressed air, which can corrode and jam pneumatic systems slowing down their operation. The presence of contaminants can also lead to system failure. Monitoring and filtering contaminants can reduce problems and improve the condition of compressed air. Early detection of these contaminants can help plant managers take preventive measures before catastrophic failures occur.

Dielectric spectroscopy has potential as a technology for detecting contaminants in compressed air. Dielectric spectroscopy is the measurement of dielectric properties of a material at multiple frequencies. The dielectric properties of a material explain the electrical interaction between the material and an electric field. Normally, this interaction depends on the frequency of the applied field and can be described best using relative complex permittivity, $\varepsilon_r = \varepsilon_r' - j\varepsilon_r''$. The real part ε_r' denotes the dielectric constant of the material and is a measure of the ability of the material to store electrical energy. The imaginary part, ε_r'', denotes the dielectric loss factor and is associated with the loss of energy in a material relative to the applied external electrical field. This relative complex permittivity of the material can be measured as a function of frequency using dielectric spectroscopy (Von Hippel, 1954a). Dielectric spectroscopy has been used for comparing different petroleum fractions (Folgero, 1998; Tjomsland, et al., 1996), sensing moisture dynamics in oil impregnated pressboard (Sheiretov & Zahn, 1995), and monitoring of moisture content and insulation degradation in oil transformers (Koch & Feser, 2004).

The goal of this project was to determine the performance of a sensor collecting dielectric spectroscopic measurements in detecting the presence of liquids, particularly water and lubricating oil, in an air stream.

Materials and Methods

Tests were performed with deionized water and lubricant oil (Sunoco Sunvis 932, Sunoco, PA). An experimental apparatus was built to produce droplets of these liquids and transport them through the dielectric sensor. Capacitance and dissipation factor of the compressed airstream with and without these droplets were measured with an impedance analyzer (model 4192 LF, Hewlett-Packard, Palo Alto, CA, USA) using a dielectric sensor. The measurements were taken over the frequencies ranging from 1MHz to 13 MHz for deionized water and 100 kHz to 13 MHz for oil sampled linearly within decades. Finally, multivariate techniques such as principal component analysis (PCA) and linear discriminant analysis (LDA) were applied for analysis of the experimentally collected data.

Experimental Apparatus Design

The experimental apparatus developed in the project consisted of three main parts. They were: 1) a mechanism to atomize liquids, 2) a test chamber to facilitate effective channeling of aerosol through the sensor, and 3) a hydraulic circuit to meter liquids into the chamber.

1) Atomizing Mechanism

Industrial hydraulic atomizing nozzles (model 1/4 LN, Spraying Systems Co., Wheaton, IL) were used to generate fine droplets of liquid contaminants that could be entrained in the airstream. These nozzles were capable of producing droplets of sizes 10 to 500 micrometers in diameter.

2) Experimental Chamber

An experimental chamber (figure 16) was built for entrainment and transport of liquid droplets through the dielectric sensor. The chamber consisted of a long PVC pipe with relatively larger diameter enclosing the spray area, and smaller PVC pipes and fittings for proper attachment with the dielectric sensor. A model of liquid droplets trajectory was developed and the simulation was used to identify the appropriate sizes of PVC parts required for the chamber. The sensor was connected collinearly with the large chamber to allow effective movement of droplets out of the sensor.

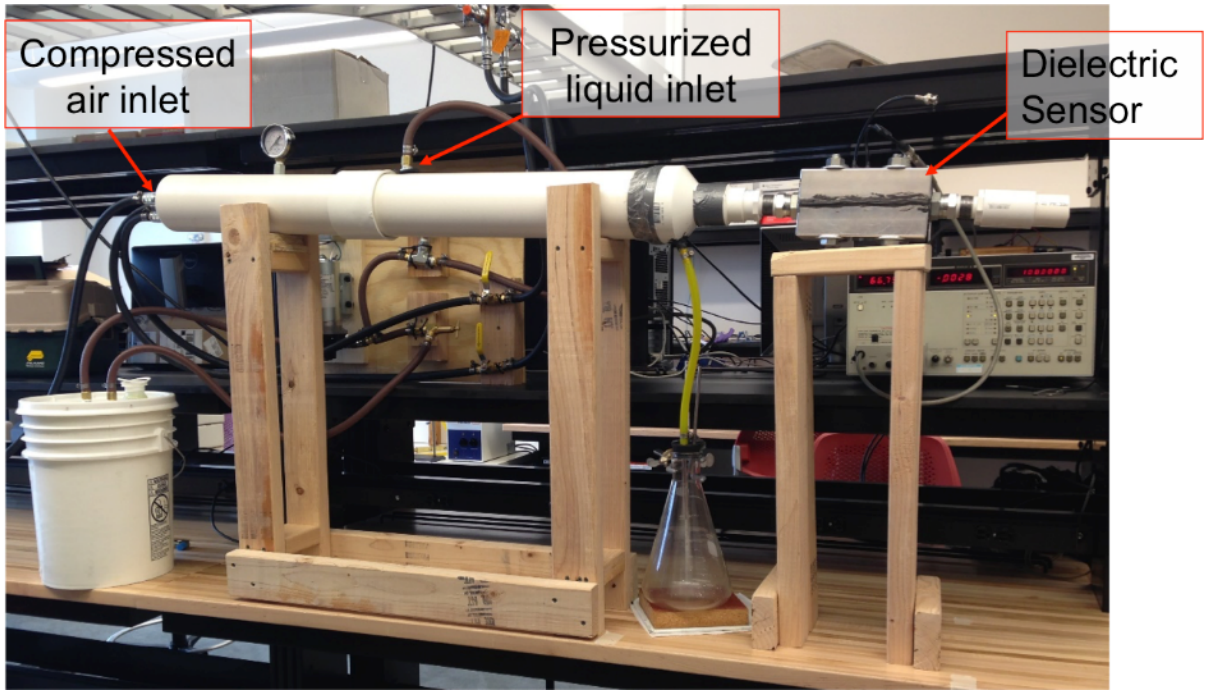

Figure 16. Experimental apparatus used for the test with deionized water shows the hydraulic circuit and impedance analyzer used for the test.

The section of the chamber enclosing spray area was selected to be four inch in diameter and consisted of two PVC pipes of different length attached by a coupler. Two pipes were used rather than a single long pipe to ease disassembly and adjustments between the tests.

The chamber had attachments for the liquid nozzle and a hose connection to a 2000 ml conical flask at the top-middle and front-bottom sections of the pipe, respectively. The 2000 ml flask was used to collect liquid from the bottom of the pipe when droplets came in contact the inner sides of the tube and coalesced. Wooden stands were built to support and adjust the orientation of the experimental chamber and sensor during the tests. The chamber was adjusted to a 10-15 degrees angle from horizontal so that the residue could easily flow to the conical flask without collecting inside the chamber.

3) Hydraulic Circuit

A hydraulic circuit was developed to meter the test fluids into the experimental chamber. The hydraulic circuit consisted of a reservoir, diaphragm pump, pressure relief valve and hydraulic hoses (Figure 17). The diaphragm pump (model 8030-863-239, Shurflo, Cypress, Ca) moved the test liquids from the reservoir to the nozzle. The pressure relief valve (model 110, Spraying Systems Co., Wheaton, IL) set the nozzle pressure to achieve the droplet characteristics and flow rate for the tests.

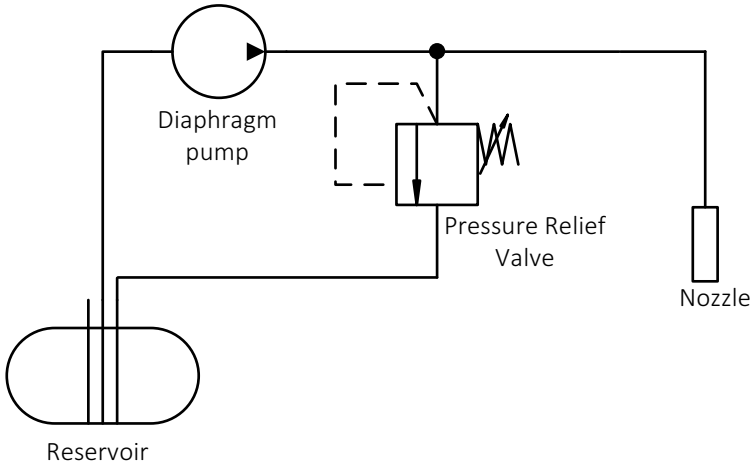

Figure 17. Schematic of hydraulic circuit used for metering liquids to the nozzle

Test Procedure

Two separate tests were conducted with: 1) deionized water and 2) air lubricating oil (Sunvis 932, Sunoco, Philadelphia, PA). These tests were conducted inside the lab where the temperature was relatively constant at 21 degrees Celsius. Compressed air available in the lab was used to transport the atomized test liquids through the sensor. The air was supplied at the rear end of the long chamber using three sources of compressed air. The effective flow rate of the air through the sensor was observed to be 40 cubic feet per minute (cfm). An impedance analyzer (model HP 4192A LF, Hewlett-Packard, Palo Alto, CA, USA) was used for taking dielectric measurements of the fluid in the sensor during these tests.

The first test for contaminants in pneumatic systems involved injecting deionized water into the air stream. A nozzle with a 0.5 capacity size was used for the tests. The 0.5 capacity size suggests that the nozzle can produce a flow rate of 0.5 gal/min (1893 ml/min) at 40 psi (276 kPa) inlet pressure. The test was replicated three times, and each replication consisted of more than 25 samples, each for spray and no-spray conditions. The impedance

analyzer measured capacitance and dissipation factor at 13 different frequencies ranging from 1 MHz to 13 MHz sampled linearly within decades. After each replication, the dielectric sensor was disassembled, cleaned and dried. This disassembly was done to avoid any possible variation in the data for different replications because of residue that may have collected inside the sensor after each test.

The second test was performed using lubricating light oil. A nozzle with a 1.5 capacity size was used for this test. A higher capacity size nozzle than that used for the water experiment was required because smaller capacity nozzles were unable to atomize the more viscous oil effectively. The test with oil also consisted of three replications, each consisting of 10 to 15 samples for spray and no-spray conditions. Unlike the test with deionized water, the experimental apparatus was not disassembled during the test with oil, and all three replications were performed sequentially at once with alternating spray and no-spray conditions. For this test, additional connectors were added at the outlet end of the dielectric sensor to channel oil droplets to collect in a container inside a fume hood. This approach prevented unwanted exhaust of oil into the air. Additionally, the response of the sensor to oil droplets was mostly unknown since all the pilot tests were conducted solely with water as the test liquid. Therefore, for the test with oil, the frequency analyzer measured capacitance and dissipation factor at 22 different frequencies ranging from 100 kHz to 13 MHz, sampled linearly within decades.

For each test, two cases were identified for data collection: spray and no spray. “Spray” represented a case in which fine liquid droplets, entrained in the compressed air, passed through the sensor. “No-spray” represented a case in which only compressed air passed through the sensor. Capacitance and dissipation factor were measured for these two

cases at multiple frequencies. These dielectric data were then statistically analyzed to find out the effectiveness of the dielectric sensor in predicting the presence of the liquid droplets in the compressed air.

Table 3. Experimental design for the test with deionized water and light oil shows the replications performed, number of samples used and the cases used for training and test sets

Tests with	Replications	Cases	Samples
Deionized Water	3	Spray	125
		No-spray	85
Light Oil	3	Spray	35
		No-spray	35

Data Analysis

Multivariate classifiers were developed to analyze the performance of spectroscopic capacitance and dissipation factor data in separating spray and no-spray cases. These spectral data were first standardized using mean centering and normalization preprocessing techniques. The data was then split into training and test datasets. The training dataset consisted of 2/3 of the samples that were randomly chosen and the remaining 1/3 of the samples were used as the test dataset. Principal component analysis (PCA) was first applied to the training dataset, and the least number of principal components (PCs) explaining the most variation in the dataset were identified. The data projected onto these principal components, also called scores, were then used to build the classifier based on linear discriminant analysis (LDA). The same lowest number of principal components was used to rotate the test dataset and generate test scores. The classifier developed from training dataset was then applied on these test scores to investigate its efficiency in predicting test cases.

Results and Discussion

The classifiers developed for the two tests were able to accurately separate the two cases: spray and no-spray. For both the tests with deionized water and oil, the first two principal components (PCs) were enough to explain 93% and 92% of the variation in the data respectively. Therefore, first two principal components were chosen for rotation of the measured dielectric data. Figure 18 and 19 show the resulting PCA scores plotted on the selected principal components for deionized water and oil respectively. The same principal components were also used to get the PCA scores of the test dataset and can be observed on figures 18 and 19 for respective tests.

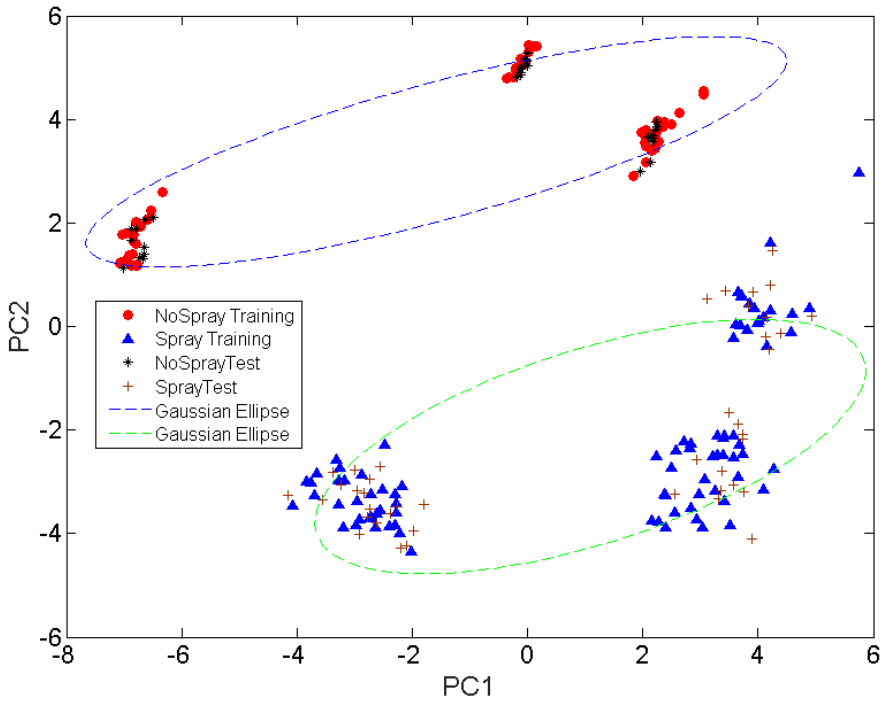

Figure 18. Dielectric spectroscopic data from the test with water projected on the first two principal components. Red and Blue data points are from training dataset while the black and brown data points are from test dataset.

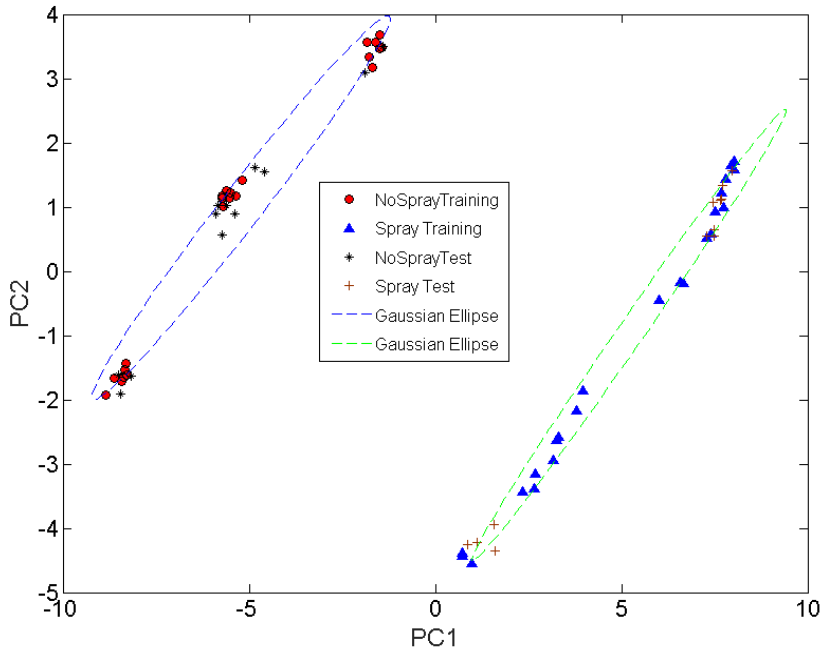

Figure 19. Dielectric spectroscopic data from the test with oil projected onto the first two principal components. Red and Blue data points are from training dataset while the black and brown data points are from test dataset.

Both these plots show that the variations in the measurements were not only due to spray and no-spray cases, but also due to differences in the replications. Since data points for spray and no-spray cases are distinctly separated in the plane formed by two principal components, a classifier developed using LDA was able to predict both training and test data accurately (Table 4 and 5).

The result from the test with deionized water (Table 4) showed that the classifier developed using the training dataset was able to predict all 57 no-spray and 83 spray cases in the training dataset accurately. This model also predicted all 28 no-spray and 42 spray cases in the test dataset.

Table 4. Misclassification table for training (left) and test (right) datasets for test with deionized water

Training Set		
	No-Spray	Spray
No-Spray	57	0
Spray	0	83

Test Set		
	No-Spray	Spray
No-Spray	28	0
Spray	0	42

Similar results were observed with light oil (Table 5). The classifier developed for the analysis was accurately predicted both cases in the training and test dataset. For the training set, the classifier predicted all no-spray and spray cases without any errors. It also accurately predicted all 12 no-spray and spray cases in the test dataset.

Table 5. Misclassification table for training (left) and test (right) datasets for test with light oil

Training Set		
	No-Spray	Spray
No-Spray	23	0
Spray	0	23

Test Set		
	No-Spray	Spray
No-Spray	12	0
Spray	0	12

These results showed that the dielectric sensor was successful in capturing the differences in dielectric properties of the air stream due to the presence and absence of liquid droplets in both the tests.

The visual inspection of the data for both the tests showed that the variation in the two cases were distinct for capacitance measurement (20a and 21a), while their variation in dissipation factor measurement was not very clear (20b and 21b). The capacitance of the sensor increased across all the frequencies when liquid droplets were entrained in the airstream. This is probably because of the increase in the effective dielectric constant of the

compressed air stream due to presence of deionized water and oil, both of which have a higher dielectric constant than air. Air has dielectric constant of 1, while deionized water and oil have dielectric constant of 80 and 3.9 respectively. Since capacitance has direct relationship with dielectric constant, the increase in dielectric constant of the compressed may have increased the capacitance measurements.

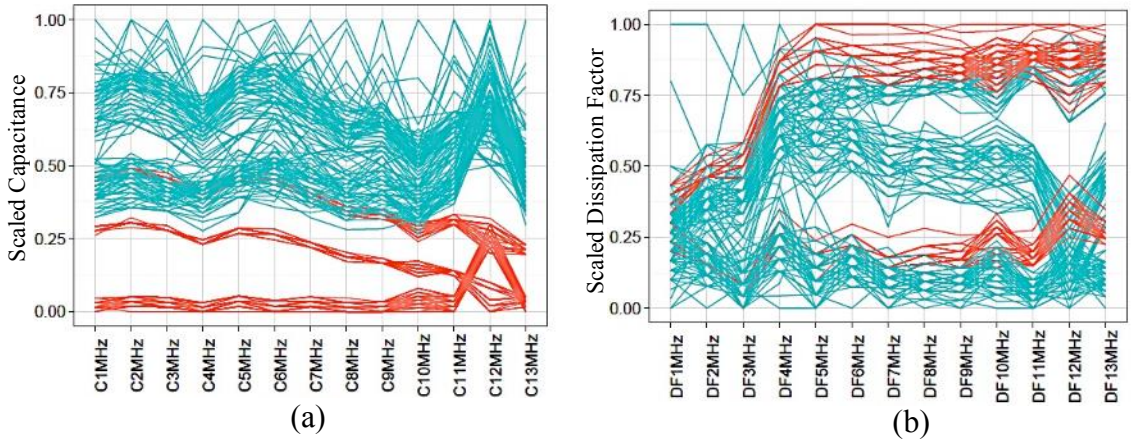

Figure 20. (a) Capacitance and (b) dissipation factor values scaled to minimum zero and maximum one for spray (blue lines) and no-spray (red lines) cases across multiple frequencies for tests with deionized water

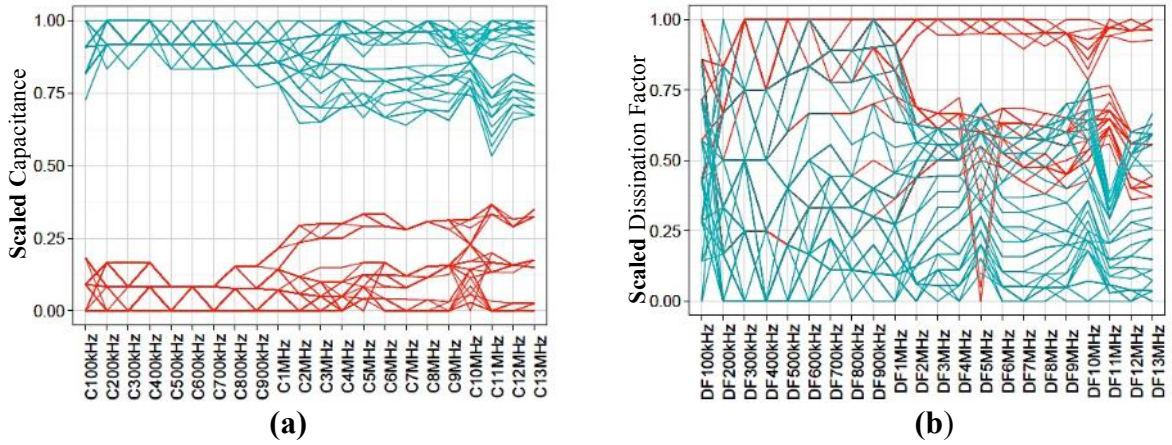

Figure 21. (a) Capacitance and (b) dissipation factor values scaled to minimum zero and maximum one for spray (blue lines) and no-spray (red lines) cases across multiple frequencies for tests with light oil

Conclusions

From this research, it can be concluded that:

1. The dielectric spectroscopic sensor can detect the presence of water and oil droplets in the compressed air.
2. At the frequencies from 100 kHz to 13 MHz, the sensor was more responsive to change in condition of the fluids tested in the project.

Acknowledgements

This project was supported by the National Fluid Power Association (NFPA) and the Iowa State Experiment Station.

REFERENCES

Davis, J. 2007. Air contamination: Is oil really the problem? Filtration and Separation, 44(4), 25–27.

Folgero, K. 1998. Broad-Band Dielectric Spectroscopy of Low Permittivity Fluids using One Measurements Cell. Instrumentation and Measurement, IEEE Transactions on, 47(4), 881-885.

Improving Compressed Air System Performance a Sourcebook for Industry. (2003). Washington, D.C: United States. Dept. of Energy.

Koch, M., and Feser, K. 2004. Reliability and Influences on Dielectric Diagnostic Methods to Evaluate the Ageing State of Oil-paper Insulations. Retrieved 05 18, 2014, from www.uni-stuttgart.de:http://www.unistuttgart.de/ieh/forschung/veroeffentlichungen/2004_aptadm_koch.pdf

National Renewable Energy Lab., Golden, CO. (US). 2003. Improving Compressed Air System Performance: A Sourcebook for Industry (No. DOE/GO-102003-1822). Retrieved from http://www.osti.gov/scitech/biblio/15006054.

Rollins, J. P. 2003. Compressed Air and Gas Institute. Englewood Cliffs: Prentice Hall.

Saidur, R., Rahim, N. A., and Hasanuzzaman, M. 2010. A review on compressed-air energy use and energy savings. Renewable and Sustainable Energy Reviews, 14(4), 1135–1153.

Shanghai, H. Q., & McKane, A. 2008. Improving Energy Efficiency of Compressed Air System Based on System Audit. Lawrence Berkeley National Laboratory. Retrieved from http://escholarship.org/uc/item/13w7f2fc

Sheiretov, Y., and Zahn, M. 1995. Dielectrometry Measurements of Moisture Dynamics in Oil-impregnated Pressboard. IEEE Transactions on Dielectrics and Electrical Insulation, 2, 329-351.

Tjomsland, T., Hilland, J., Christy, A. A., Sjoblom, J., Riis, M., Friis, T., and Folgero, K. 1996. Comparison of Infrared and Impedance Spectra of Petroleum Fractions. Fuel, 75(3), 322-332.

US Department of Energy. August 2004. Determine the Cost of Compressed Air for Your Plant, Compressed Air Tip Sheet #1, DOE/GO-102004-1926

Von Hippel, A. R. 1954a. Dielectric Materials and Applications. New York: The Technology Press of M.I.T and John Wiley and Sons.

CHAPTER 5. GENERAL CONCLUSIONS

General Discussion

The research investigating dielectric sensing of particle contaminants in a hydraulic fluid, as discussed in chapter 3, shows that the dielectric sensor developed in the research project determined different levels of iron powder and ISO test dust in the moving hydraulic fluid with good accuracy using dielectric spectroscopy. The results show that the dielectric sensor performed better when a larger diameter central rod was used to measure iron powder in the hydraulic fluid. This improved performance is likely because the larger diameter of the rod increased the sensing capacitance of the dielectric sensor, and thus the measurements were less affected by stray capacitances. Similarly, it can be observed that the sensor had better sensitivity to iron powder than the ISO test dust (mostly silicon dioxide) for the same central rod. Thus, the dielectric sensor may have better ability to detect metallic contaminants in hydraulic fluids.

Based on the results from pneumatics research described in chapter 4, it can be concluded that dielectric spectroscopy has the potential to detect the presence of entrained water and oil droplets in a compressed airstream. The same dielectric spectroscopic sensor developed in the hydraulic research was used for this research. The statistical analysis showed the two cases (airstream with and without liquid droplets) could be separated using dielectric spectroscopic data. This result shows that the dielectric sensor has the ability to capture variation in compressed air due to the inclusion of liquid contaminants.

Both of these investigations show that the dielectric spectroscopic sensor can provide valuable assessments of fluid contamination.

Recommendations for Future Research

The research work discussed in chapter 3 and 4 were performed with a laboratory instrument (HP 4192A LF Impedance Analyzer), which uses auto-balancing bridge technique to measure impedances. In the future, an electronic unit that uses similar auto-balancing bridge technique can be developed for the dielectric sensor, so that the sensor can work as stand-alone device. Since the current design of the dielectric sensor cannot be used for auto-balancing bridge measurement, the design of sensor's central rod should be modified to accommodate another circuit.

In the research with hydraulic fluid, a mineral-based hydraulic fluid (Shell Tellus ISO VG 46) was used for all the tests. In the future, tests could be conducted to investigate performance of dielectric sensor in detecting contaminants in other types of hydraulic fluids, such as vegetable oil-based or synthetic hydraulic fluids. Similarly, test should be performed to examine the efficacy of dielectric spectroscopy in determining different types of contaminants and their level when mixed in hydraulic fluids.

For the test with hydraulic fluid, the temperature and flow rate of the fluid were kept constant. Since these parameters can affect dielectric measurement of the sensor, tests should be performed to investigate how these measurements vary with different fluid temperatures and flow rates. Statistical models from these tests could be later used to calibrate the dielectric sensor for detecting contamination of fluid at different temperature and flow rate conditions.

In the test with compressed air, the temperature may have some influence on the dielectric measurement. Tests can be performed to investigate the effect of temperature on dielectric sensor readings, which can be later used for temperature correction of the sensor.

Furthermore, a test can be developed in which the dielectric sensor can be calibrated to read different volume fractions of water and oil droplets in the compressed airstream.

APPENDIX. MECHANICAL DRAWINGS OF DIELECTRIC SPECTROSCOPIC SENSOR

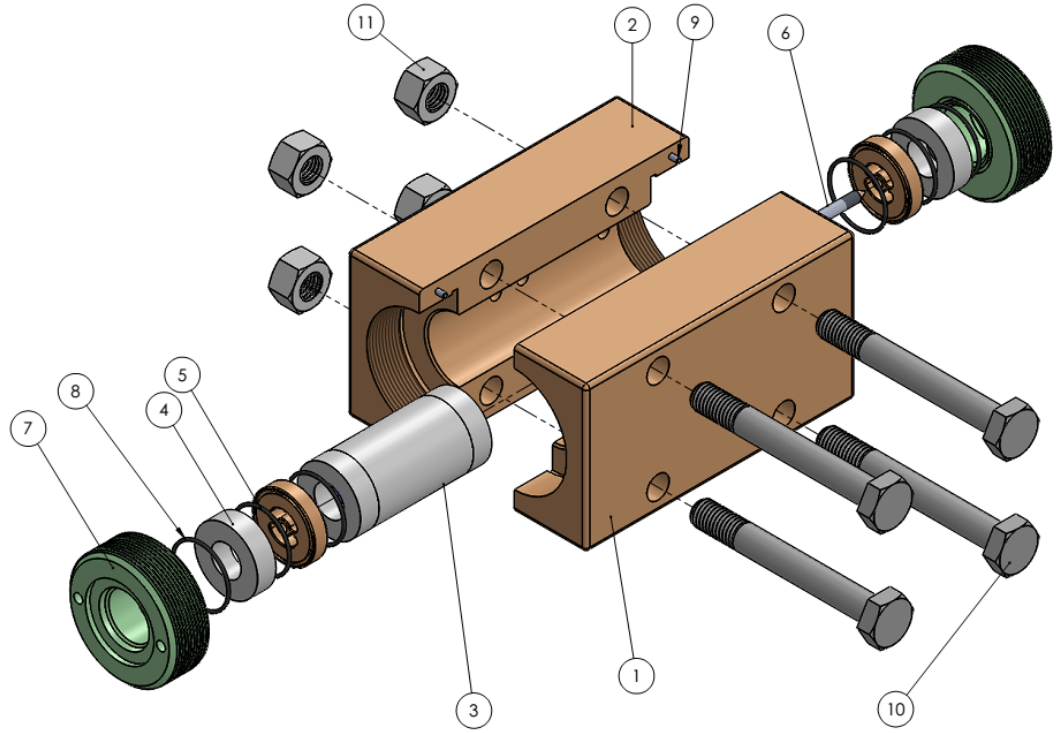

ITEM NO.	PART NUMBER	DESCRIPTION	QTY.
1	002-0010	Sensor Housing Half	1
2	002-0011	Sensor Housing modified Half	1
3	001-SA-0002	Electrode and Shield Assembly	1
4	002-0007	Insulating Ring	2
5	002-0008	Rod Holder	2
6	002-0009	Central Electrode	1
7	002-0012	Adaptor for hydraulic tube connection	2
8	003-0001	O-Ring (AS568A-029)	6
9	003-0005	Dowel pin	4
10	003-0002	Bolt	4
11	003-0003	Nut	4

UNLESS OTHERWISE SPECIFIED:
DIMENSIONS ARE IN INCHES
TOLERANCES:
FRACTIONAL ±
ANGULAR: MACH ± BEND ±
TWO PLACE DECIMAL ±
THREE PLACE DECIMAL ±
INTERPRET GEOMETRIC TOLERANCING PER:
MATERIAL
FINISH
NEXT ASSY | USED ON
APPLICATION | DO NOT SCALE DRAWING

	NAME	DATE
DRAWN	SK	
CHECKED		
ENG APPR.		
MFG APPR.		
Q.A.		
COMMENTS:		

PROPRIETARY AND CONFIDENTIAL
THE INFORMATION CONTAINED IN THIS DRAWING IS THE SOLE PROPERTY OF <IOWA STATE UNIVERSITY>. ANY REPRODUCTION IN PART OR AS A WHOLE WITHOUT THE WRITTEN PERMISSION OF <IOWA STATE UNIVERSITY> IS PROHIBITED.

Dielectric Sensor

TITLE: Capacitive Load Sensing Assembly

SIZE	DWG. NO.	REV
B	001-A-0001	

SCALE: 1:2 | WEIGHT: | SHEET 1 OF 1

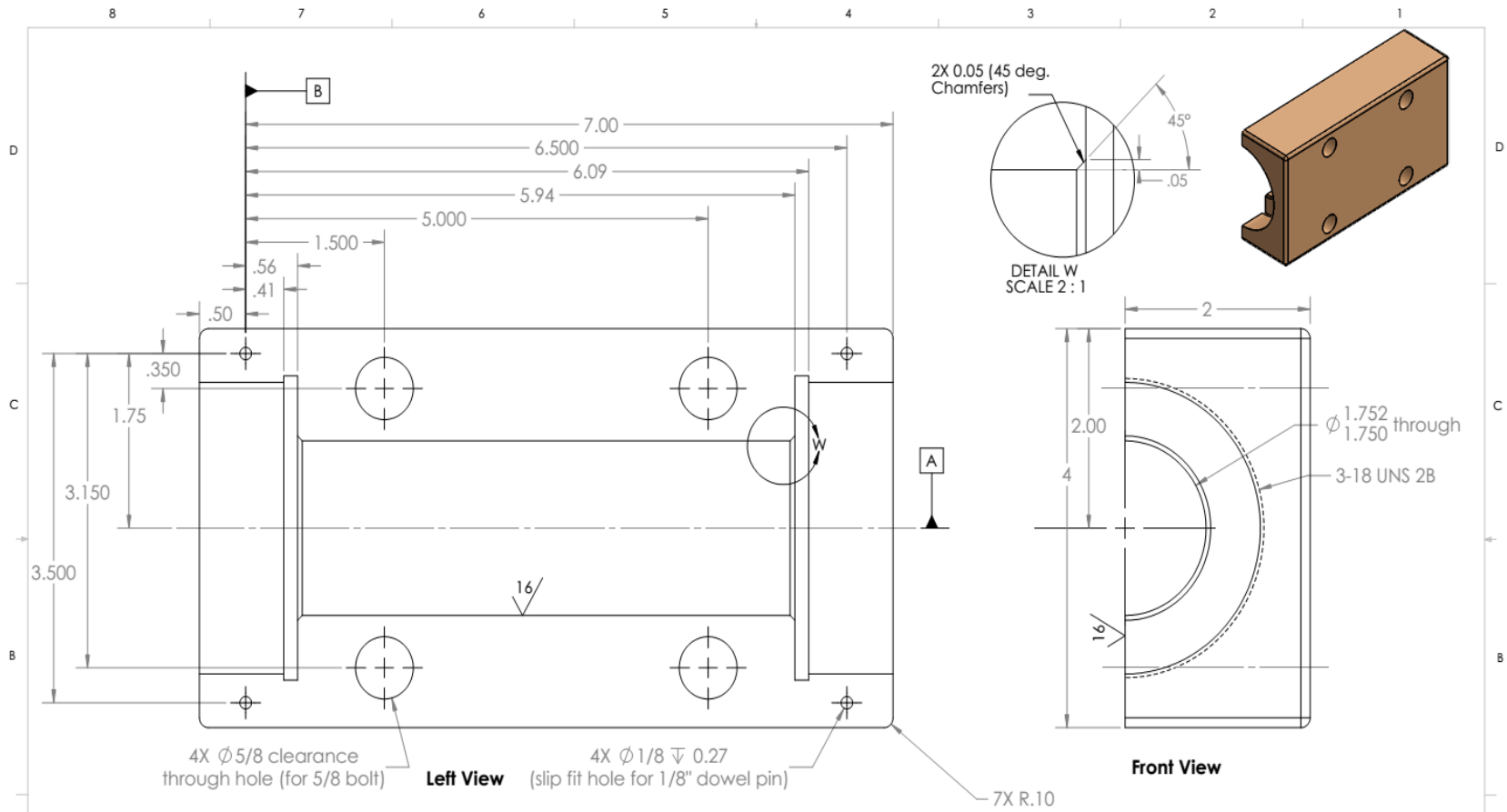

Note:

Two rectangular(7.5in. X 4 in. X 2 in.) aluminum blocks will be used to manufacture a housing for the sensor, and it involves following steps:

1. Holes for bolts and dowel pins should be made on each block
2. Then, the two blocks should fastened together with nuts and bolts, and finally1.75 in. diameter (through all) hole and 3-18UNS tapped hole should be made on 4in. X 4in. face (formed after fastening).

		UNLESS OTHERWISE SPECIFIED:		NAME	DATE
		DIMENSIONS ARE IN INCHES TOLERANCES: FRACTIONAL ± ANGULAR: MACH ± BEND ± TWO PLACE DECIMAL ±0.01 THREE PLACE DECIMAL ±0.001	DRAWN	SK	
			CHECKED		
			ENG APPR.		
			MFG APPR.		
			Q.A.		
			COMMENTS:		
		INTERPRET GEOMETRIC TOLERANCING PER:			
		MATERIAL 2024-T3			
NEXT ASSY	USED ON	FINISH			
APPLICATION		DO NOT SCALE DRAWING			

Dielectric Sensor

TITLE: Sensor Housing Half

SIZE	DWG. NO.	REV
B	002-0010	

SCALE: .75:1 WEIGHT: SHEET 1 OF 1

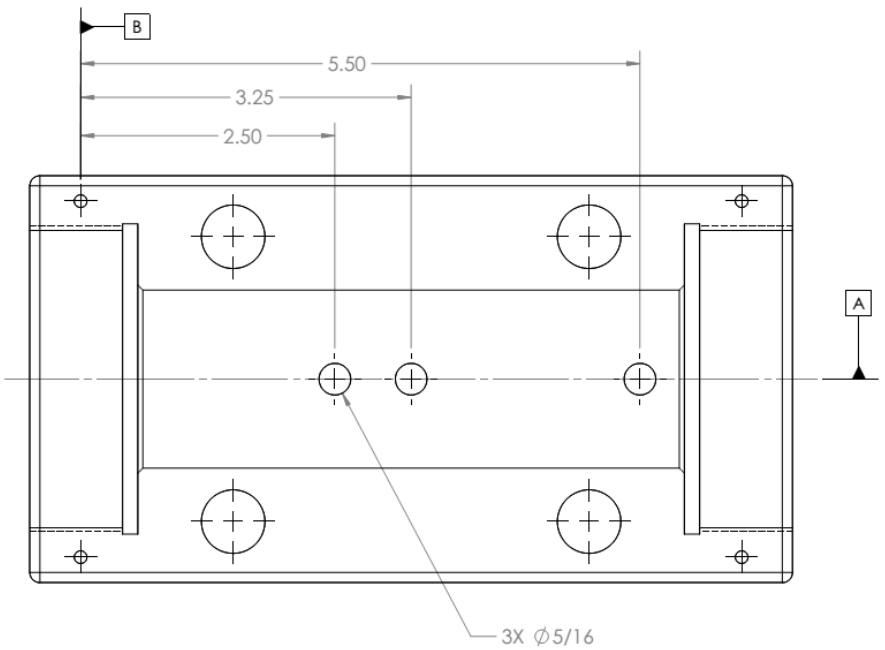

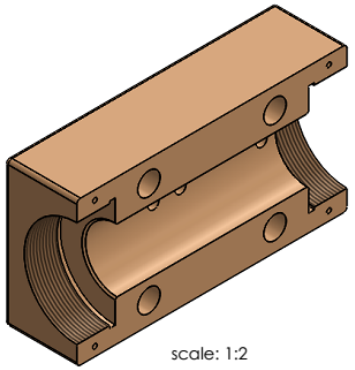

scale: 1:2

Note:

This part (002-0011) is a modified part 002-0010 with three holes. So dimensions in part 002-0010 should be used as reference to make this part.

		UNLESS OTHERWISE SPECIFIED:		NAME	DATE
		DIMENSIONS ARE IN INCHES TOLERANCES: FRACTIONAL ± ANGULAR: MACH ± BEND ± TWO PLACE DECIMAL ±0.01 THREE PLACE DECIMAL ±	DRAWN	SK	
			CHECKED		
			ENG APPR.		
			MFG APPR.		
			Q.A.		
		INTERPRET GEOMETRIC TOLERANCING PER:	COMMENTS:		
		MATERIAL 2024-T3			
NEXT ASSY	USED ON	FINISH			
APPLICATION		DO NOT SCALE DRAWING			

PROPRIETARY AND CONFIDENTIAL

THE INFORMATION CONTAINED IN THIS DRAWING IS THE SOLE PROPERTY OF <IOWA STATE UNIVERSITY>. ANY REPRODUCTION IN PART OR AS A WHOLE WITHOUT THE WRITTEN PERMISSION OF <IOWA STATE UNIVERSITY> IS PROHIBITED.

Dielectric Sensor

TITLE: Sensor Housing Modified Half

SIZE	DWG. NO.	REV
B	002-0011	

SCALE: 1:1 | WEIGHT: | SHEET 1 OF 1

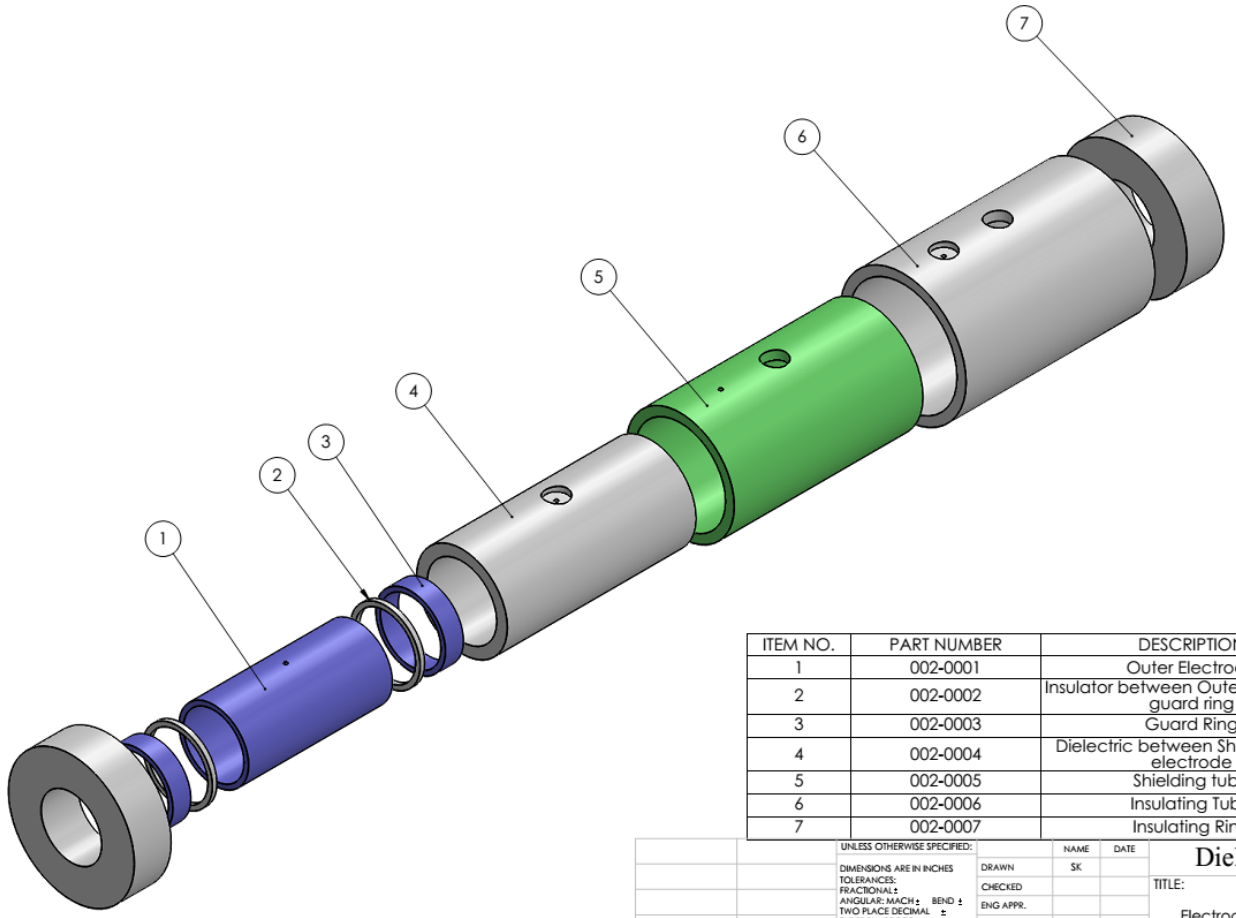

ITEM NO.	PART NUMBER	DESCRIPTION	QTY.
1	002-0001	Outer Electrode	1
2	002-0002	Insulator between Outer Electrode - guard ring	2
3	002-0003	Guard Ring	2
4	002-0004	Dielectric between Shield - Outer electrode	1
5	002-0005	Shielding tube	1
6	002-0006	Insulating Tube	1
7	002-0007	Insulating Ring	2

UNLESS OTHERWISE SPECIFIED:
DIMENSIONS ARE IN INCHES
TOLERANCES:
FRACTIONAL ±
ANGULAR: MACH ± BEND ±
TWO PLACE DECIMAL ±
THREE PLACE DECIMAL ±
INTERPRET GEOMETRIC TOLERANCING PER:
MATERIAL
FINISH
DO NOT SCALE DRAWING

	NAME	DATE
DRAWN	SK	
CHECKED		
ENG APPR.		
MFG APPR.		
Q.A.		

COMMENTS:

NEXT ASSY | USED ON
APPLICATION

Dielectric Sensor

TITLE:
Electrode and Shield Assembly

SIZE	DWG. NO.	REV
B	001-SA-0002	

SCALE: 1:1 | WEIGHT: | SHEET 1 OF 8

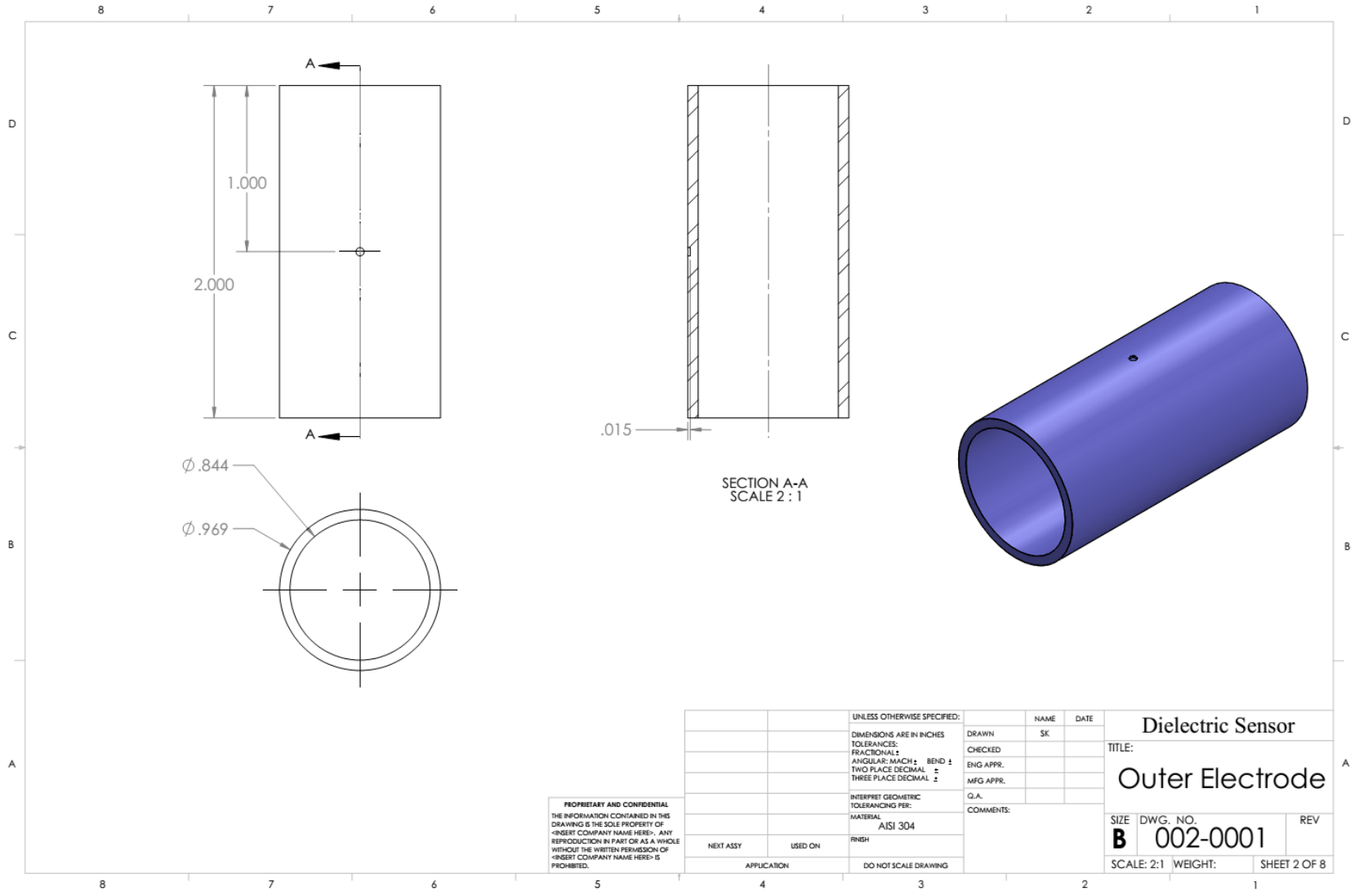
A
1.000
2.000
A
Ø.844
Ø.969
.015
SECTION A-A
SCALE 2 : 1
Dielectric Sensor
TITLE:
Outer Electrode
DWG. NO.
002-0001
SIZE
B
REV
SCALE: 2:1
WEIGHT:
SHEET 2 OF 8
UNLESS OTHERWISE SPECIFIED:
DIMENSIONS ARE IN INCHES
TOLERANCES:
FRACTIONAL ±
ANGULAR: MACH ± BEND ±
TWO PLACE DECIMAL ±
THREE PLACE DECIMAL ±
INTERPRET GEOMETRIC TOLERANCING PER:
MATERIAL
AISI 304
FINISH
DO NOT SCALE DRAWING
NAME
DATE
DRAWN
SK
CHECKED
ENG APPR.
MFG APPR.
Q.A.
COMMENTS:
NEXT ASSY
USED ON
APPLICATION
PROPRIETARY AND CONFIDENTIAL
THE INFORMATION CONTAINED IN THIS DRAWING IS THE SOLE PROPERTY OF <INSERT COMPANY NAME HERE>. ANY REPRODUCTION IN PART OR AS A WHOLE WITHOUT THE WRITTEN PERMISSION OF <INSERT COMPANY NAME HERE> IS PROHIBITED.

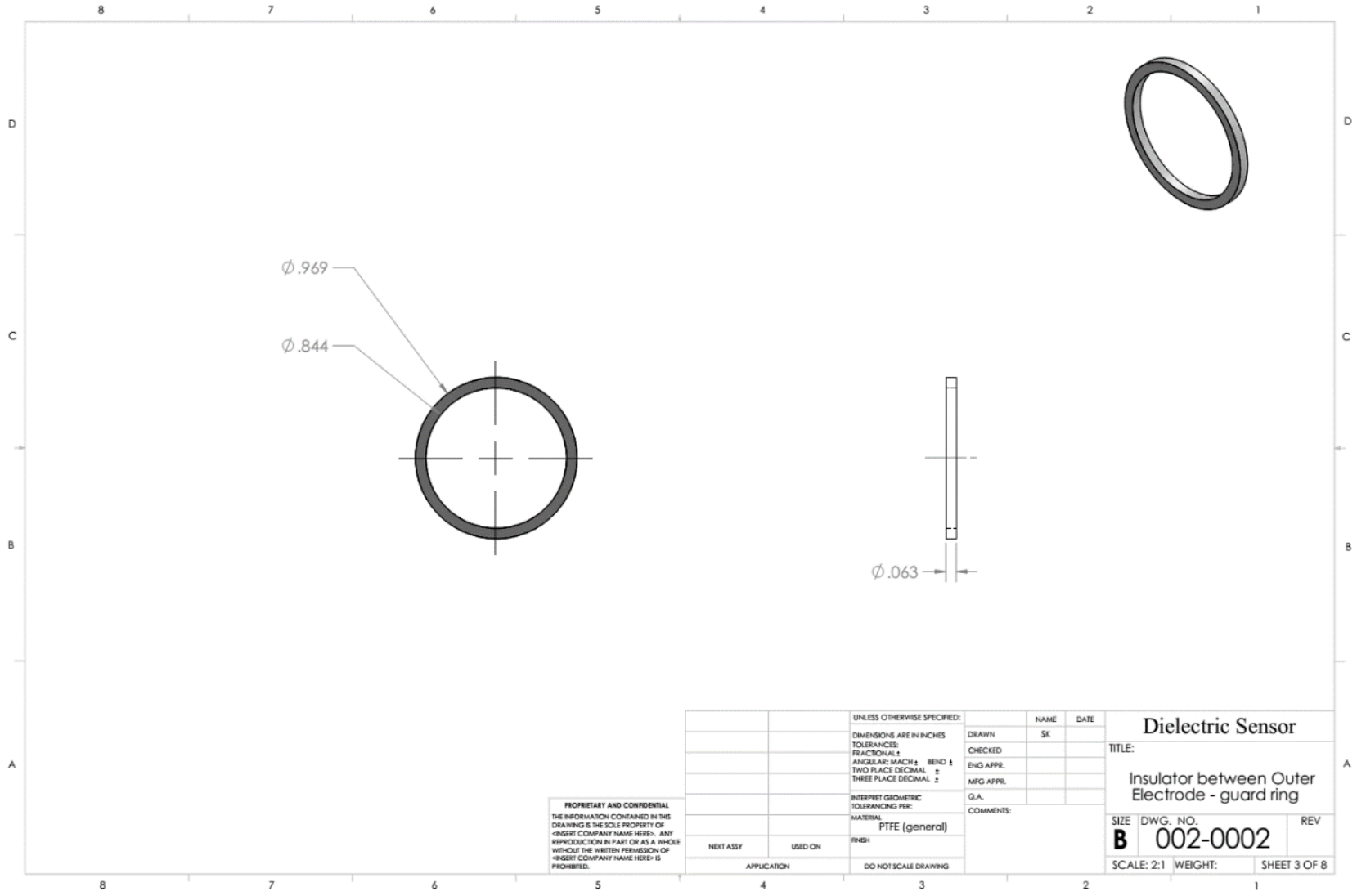

		UNLESS OTHERWISE SPECIFIED:		NAME	DATE
		DIMENSIONS ARE IN INCHES TOLERANCES: FRACTIONAL ± ANGULAR: MACH ± BEND ± TWO PLACE DECIMAL ± THREE PLACE DECIMAL ±	DRAWN	SK	
			CHECKED		
			ENG APPR.		
			MFG APPR.		
		INTERPRET GEOMETRIC TOLERANCING PER:	Q.A.		
		MATERIAL PTFE (general)	COMMENTS:		
NEXT ASSY	USED ON	FINISH			
APPLICATION		DO NOT SCALE DRAWING			

Dielectric Sensor

TITLE:

Insulator between Outer Electrode - guard ring

SIZE	DWG. NO.	REV
B	002-0002	

SCALE: 2:1 | WEIGHT: | SHEET 3 OF 8

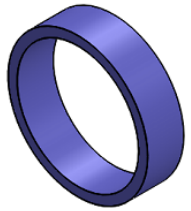

Scale: 2:1

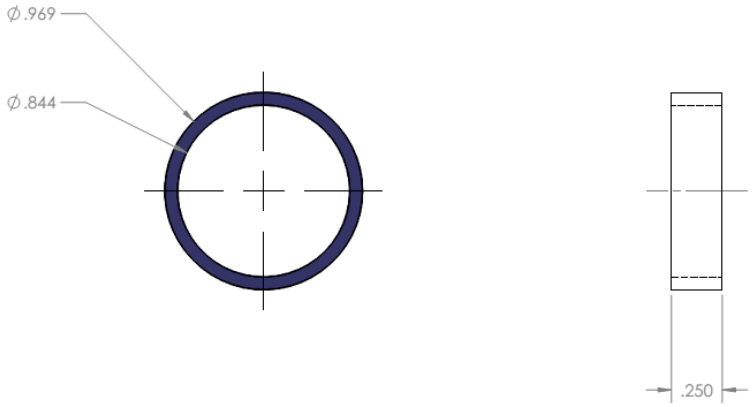

		UNLESS OTHERWISE SPECIFIED:		NAME	DATE
		DIMENSIONS ARE IN INCHES TOLERANCES: FRACTIONAL ± ANGULAR: MACH ± BEND ± TWO PLACE DECIMAL ± THREE PLACE DECIMAL ±	DRAWN	SK	
			CHECKED		
			ENG APPR.		
			MFG APPR.		
		INTERPRET GEOMETRIC TOLERANCING PER:	Q.A.		
		MATERIAL AISI 304	COMMENTS:		
NEXT ASSY	USED ON	FINISH			
APPLICATION		DO NOT SCALE DRAWING			

Dielectric Sensor

TITLE:

Guard Ring

SIZE	DWG. NO.	REV
B	002-0003	
SCALE: 2:1	WEIGHT:	SHEET 4 OF 8

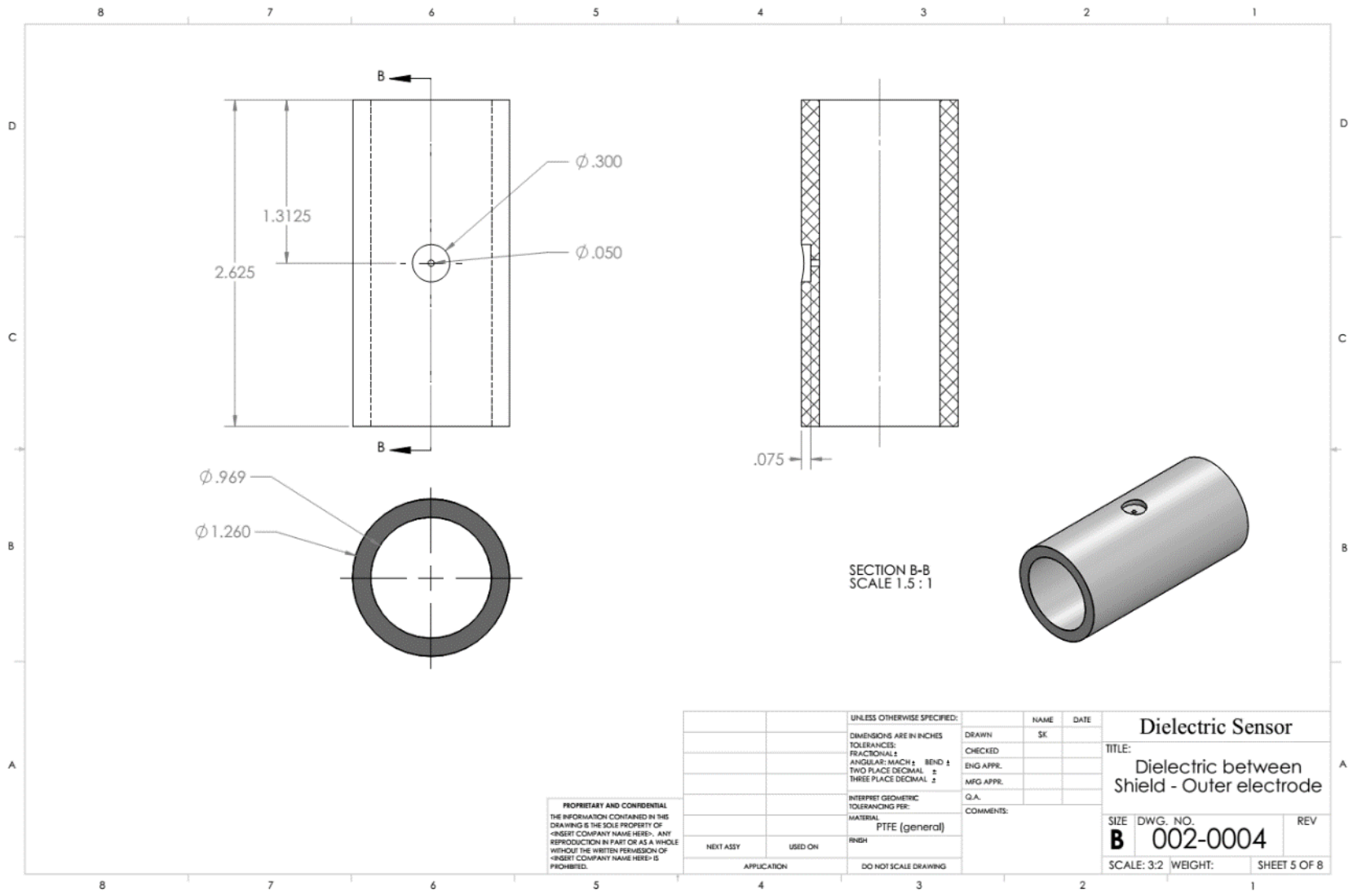
B
1.3125
2.625
Ø.300
Ø.050
B
Ø.969
Ø1.260
.075
SECTION B-B
SCALE 1.5 : 1
UNLESS OTHERWISE SPECIFIED:
DIMENSIONS ARE IN INCHES
TOLERANCES:
FRACTIONAL ±
ANGULAR: MACH ± BEND ±
TWO PLACE DECIMAL ±
THREE PLACE DECIMAL ±
INTERPRET GEOMETRIC TOLERANCING PER:
MATERIAL
PTFE (general)
FINISH
DO NOT SCALE DRAWING
NEXT ASSY
USED ON
APPLICATION
NAME
DATE
DRAWN
SK
CHECKED
ENG APPR.
MFG APPR.
Q.A.
COMMENTS:
Dielectric Sensor
TITLE:
Dielectric between Shield - Outer electrode
SIZE
B
DWG. NO.
002-0004
REV
SCALE: 3:2
WEIGHT:
SHEET 5 OF 8
PROPRIETARY AND CONFIDENTIAL
THE INFORMATION CONTAINED IN THIS DRAWING IS THE SOLE PROPERTY OF <INSERT COMPANY NAME HERE>. ANY REPRODUCTION IN PART OR AS A WHOLE WITHOUT THE WRITTEN PERMISSION OF <INSERT COMPANY NAME HERE> IS PROHIBITED.

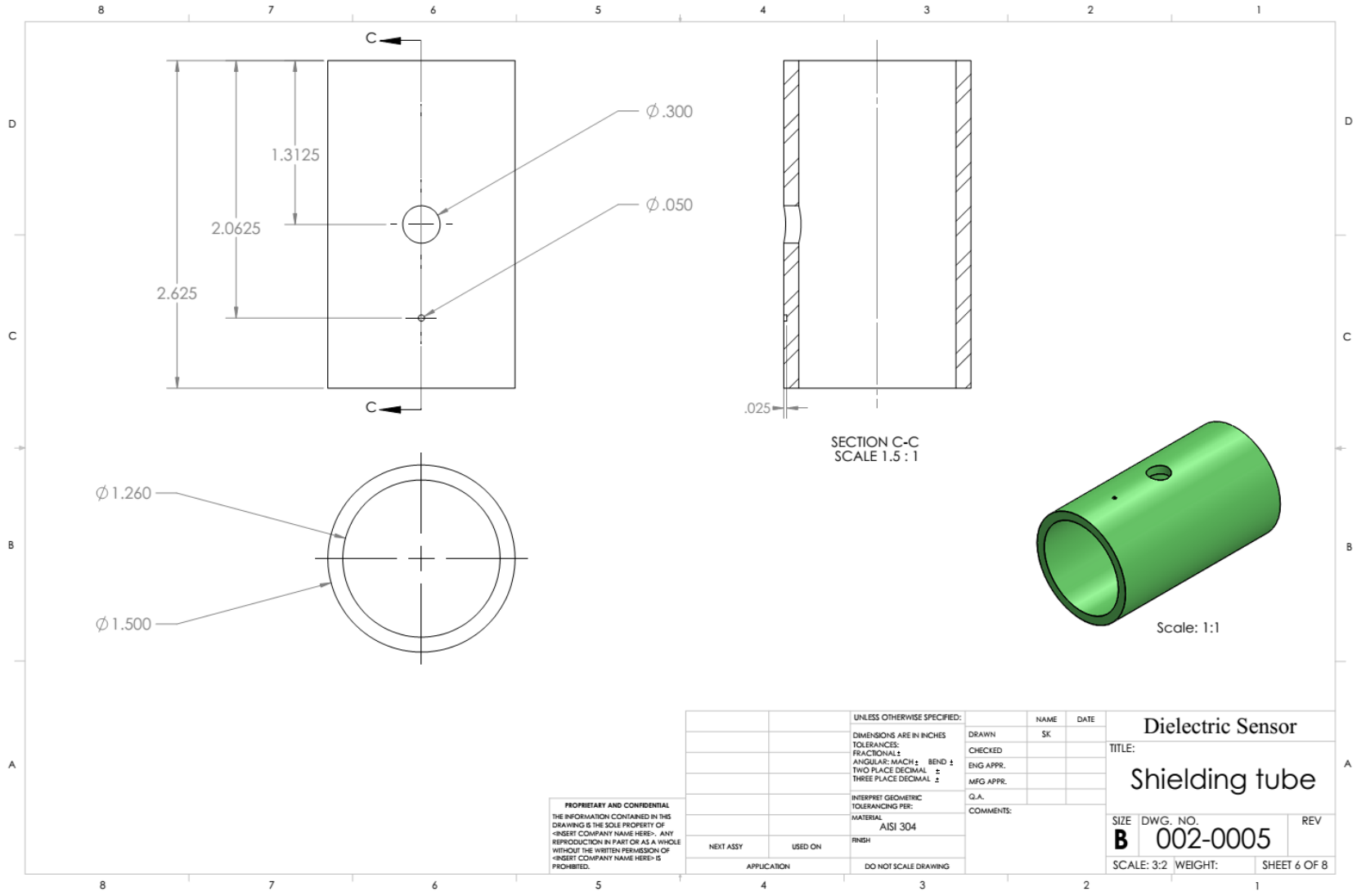
C
C
1.3125
2.0625
2.625
Ø.300
Ø.050
.025
SECTION C-C
SCALE 1.5 : 1
Ø1.260
Ø1.500
Scale: 1:1
UNLESS OTHERWISE SPECIFIED:
DIMENSIONS ARE IN INCHES
TOLERANCES:
FRACTIONAL ±
ANGULAR: MACH ± BEND ±
TWO PLACE DECIMAL ±
THREE PLACE DECIMAL ±
INTERPRET GEOMETRIC TOLERANCING PER:
MATERIAL
AISI 304
FINISH
DO NOT SCALE DRAWING
NEXT ASSY
USED ON
APPLICATION
NAME
DATE
DRAWN
SK
CHECKED
ENG APPR.
MFG APPR.
Q.A.
COMMENTS:
PROPRIETARY AND CONFIDENTIAL
THE INFORMATION CONTAINED IN THIS DRAWING IS THE SOLE PROPERTY OF <INSERT COMPANY NAME HERE>. ANY REPRODUCTION IN PART OR AS A WHOLE WITHOUT THE WRITTEN PERMISSION OF <INSERT COMPANY NAME HERE> IS PROHIBITED.
Dielectric Sensor
TITLE:
Shielding tube
SIZE
B
DWG. NO.
002-0005
REV
SCALE: 3:2
WEIGHT:
SHEET 6 OF 8

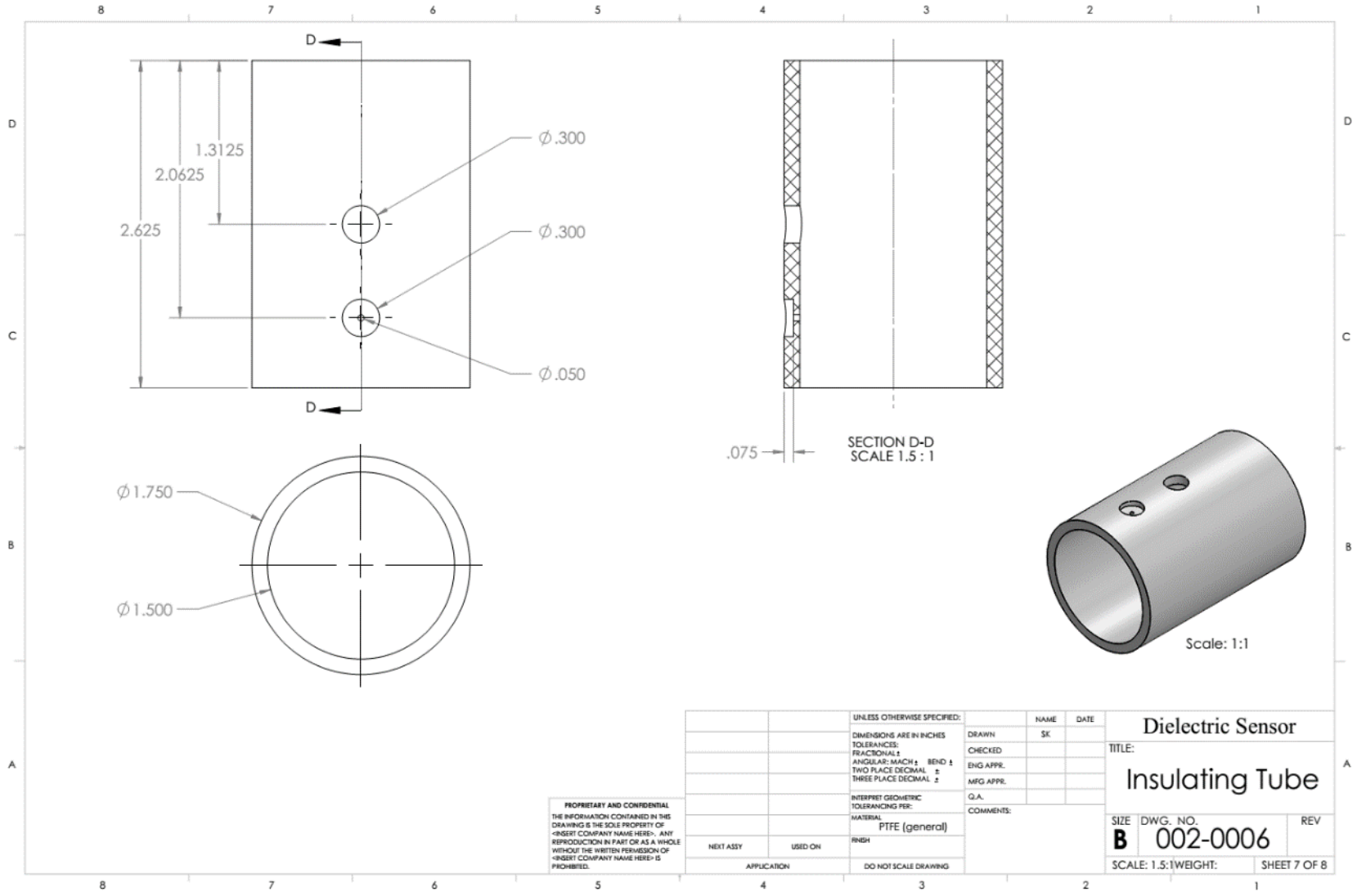
D
1.3125
2.0625
2.625
Ø.300
Ø.300
Ø.050
D
Ø1.750
Ø1.500
.075
SECTION D-D
SCALE 1.5 : 1
Scale: 1:1
UNLESS OTHERWISE SPECIFIED:
DIMENSIONS ARE IN INCHES
TOLERANCES:
FRACTIONAL ±
ANGULAR: MACH ± BEND ±
TWO PLACE DECIMAL ±
THREE PLACE DECIMAL ±
INTERPRET GEOMETRIC TOLERANCING PER:
MATERIAL
PTFE (general)
FINISH
DO NOT SCALE DRAWING
NEXT ASSY
USED ON
APPLICATION
NAME
DATE
DRAWN
SK
CHECKED
ENG APPR.
MFG APPR.
Q.A.
COMMENTS:
Dielectric Sensor
TITLE:
Insulating Tube
SIZE
B
DWG. NO.
002-0006
REV
SCALE: 1.5:1
WEIGHT:
SHEET 7 OF 8
PROPRIETARY AND CONFIDENTIAL
THE INFORMATION CONTAINED IN THIS DRAWING IS THE SOLE PROPERTY OF <INSERT COMPANY NAME HERE>. ANY REPRODUCTION IN PART OR AS A WHOLE WITHOUT THE WRITTEN PERMISSION OF <INSERT COMPANY NAME HERE> IS PROHIBITED.

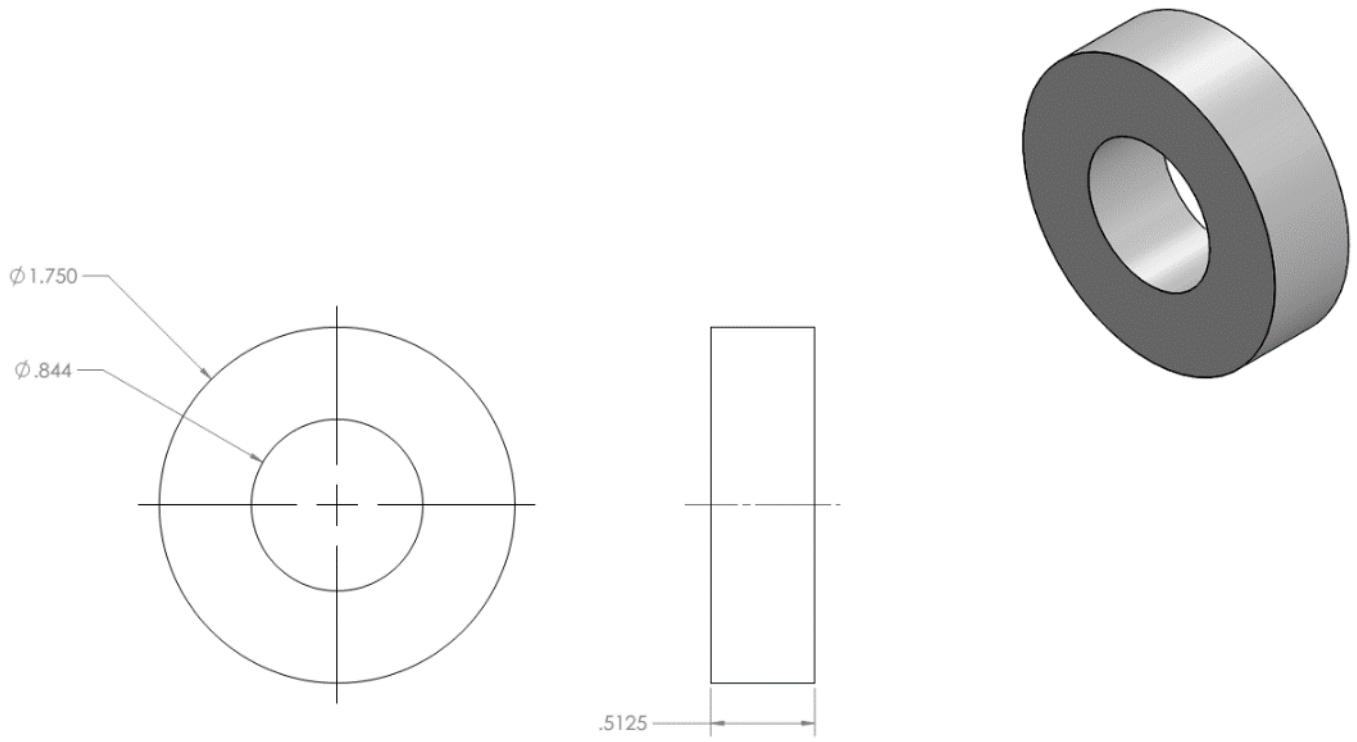

		UNLESS OTHERWISE SPECIFIED:		NAME	DATE
		DIMENSIONS ARE IN INCHES TOLERANCES: FRACTIONAL ± ANGULAR: MACH ± BEND ± TWO PLACE DECIMAL ± THREE PLACE DECIMAL ±	DRAWN	SK	
			CHECKED		
			ENG APPR.		
			MFG APPR.		
		INTERPRET GEOMETRIC TOLERANCING PER:	Q.A.		
		MATERIAL PTFE (general)	COMMENTS:		
NEXT ASSY	USED ON	FINISH			
APPLICATION		DO NOT SCALE DRAWING			

PROPRIETARY AND CONFIDENTIAL

THE INFORMATION CONTAINED IN THIS DRAWING IS THE SOLE PROPERTY OF <INSERT COMPANY NAME HERE>. ANY REPRODUCTION IN PART OR AS A WHOLE WITHOUT THE WRITTEN PERMISSION OF <INSERT COMPANY NAME HERE> IS PROHIBITED.

Dielectric Sensor

TITLE:

Insulating Ring

SIZE	DWG. NO.	REV
B	002-0007	

SCALE: 2:1 | WEIGHT: | SHEET 8 OF 8

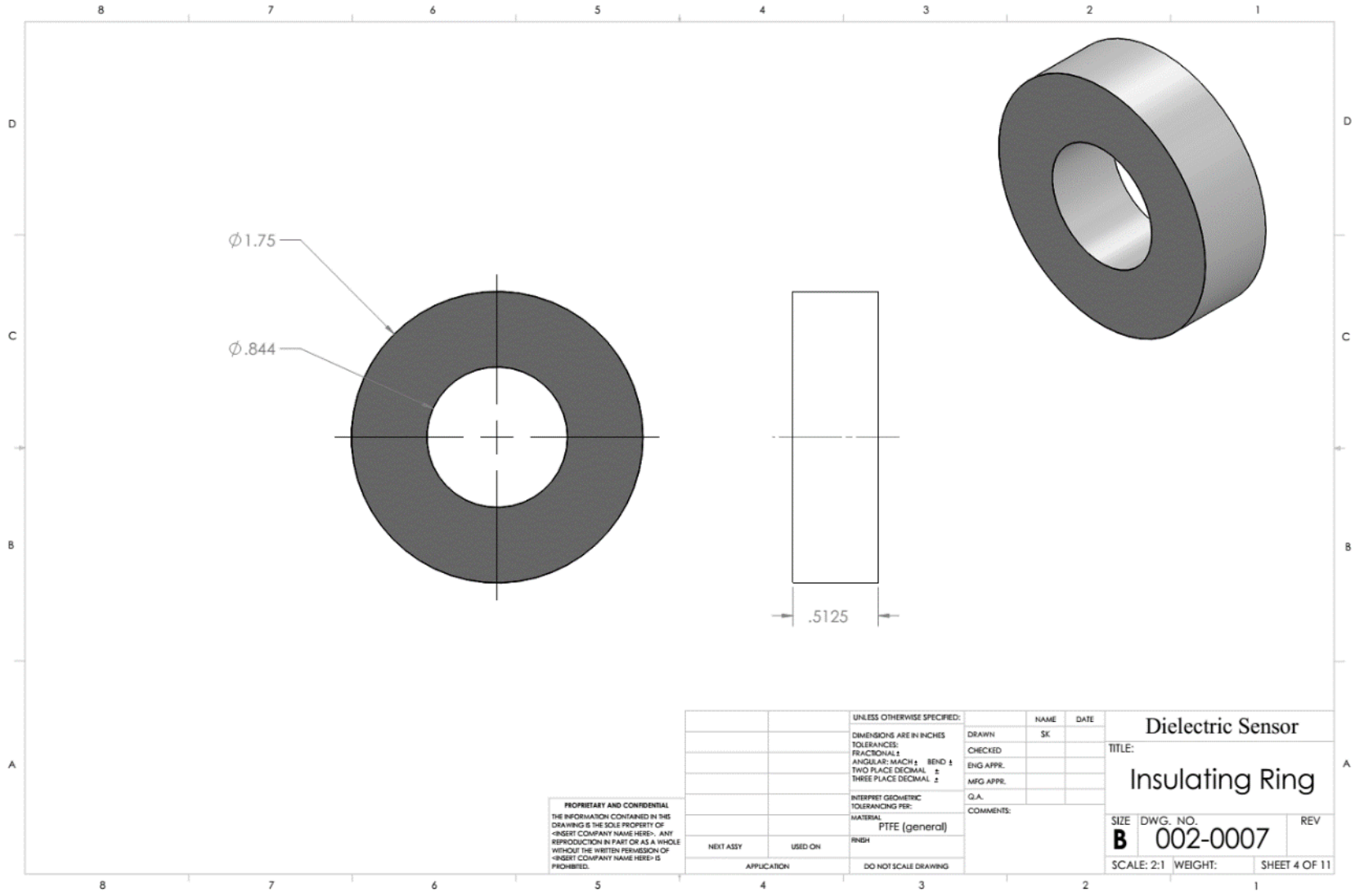

		UNLESS OTHERWISE SPECIFIED:		NAME	DATE
		DIMENSIONS ARE IN INCHES TOLERANCES: FRACTIONAL ± ANGULAR: MACH ± BEND ± TWO PLACE DECIMAL ± THREE PLACE DECIMAL ±	DRAWN	SK	
			CHECKED		
			ENG APPR.		
			MFG APPR.		
		INTERPRET GEOMETRIC TOLERANCING PER:	Q.A.		
		MATERIAL PTFE (general)	COMMENTS:		
NEXT ASSY	USED ON	FINISH			
APPLICATION		DO NOT SCALE DRAWING			

PROPRIETARY AND CONFIDENTIAL

THE INFORMATION CONTAINED IN THIS DRAWING IS THE SOLE PROPERTY OF <INSERT COMPANY NAME HERE>. ANY REPRODUCTION IN PART OR AS A WHOLE WITHOUT THE WRITTEN PERMISSION OF <INSERT COMPANY NAME HERE> IS PROHIBITED.

Dielectric Sensor

TITLE:

Insulating Ring

SIZE	DWG. NO.	REV
B	002-0007	

SCALE: 2:1 | WEIGHT: | SHEET 4 OF 11

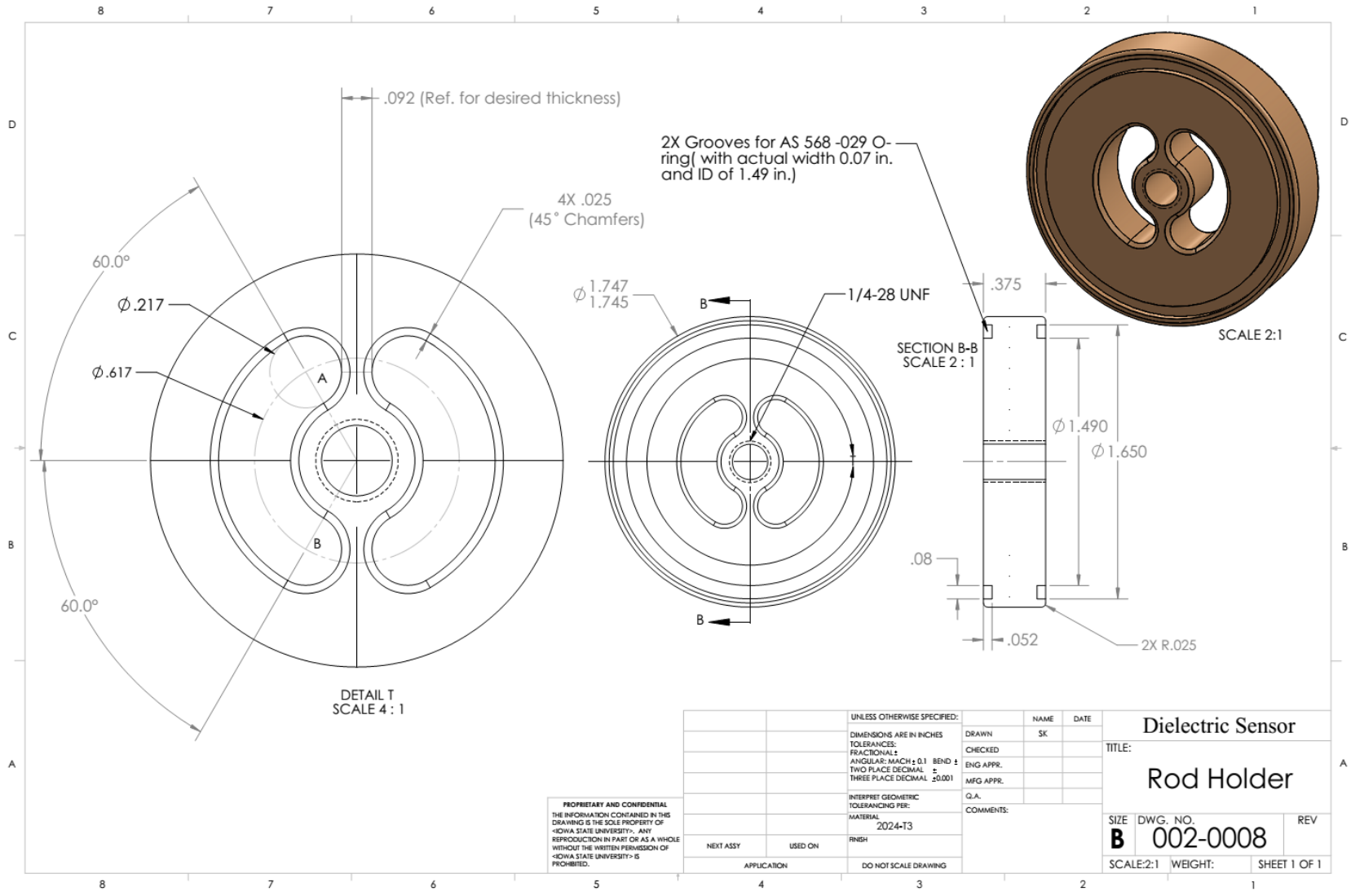
.092 (Ref. for desired thickness)
2X Grooves for AS 568 -029 O-ring(with actual width 0.07 in. and ID of 1.49 in.)
4X .025 (45° Chamfers)
60.0°
Ø.217
Ø.617
A
B
60.0°
DETAIL T
SCALE 4 : 1
Ø1.747
1.745
B
1/4-28 UNF
B
.375
SECTION B-B
SCALE 2 : 1
Ø1.490
Ø1.650
.08
.052
2X R.025
SCALE 2:1
UNLESS OTHERWISE SPECIFIED:
DIMENSIONS ARE IN INCHES
TOLERANCES:
FRACTIONAL ±
ANGULAR: MACH ± 0.1 BEND ±
TWO PLACE DECIMAL ±
THREE PLACE DECIMAL ±0.001
INTERPRET GEOMETRIC TOLERANCING PER:
MATERIAL
2024-T3
FINISH
DO NOT SCALE DRAWING
NAME
DATE
DRAWN
SK
CHECKED
ENG APPR.
MFG APPR.
Q.A.
COMMENTS:
NEXT ASSY
USED ON
APPLICATION
PROPRIETARY AND CONFIDENTIAL
THE INFORMATION CONTAINED IN THIS DRAWING IS THE SOLE PROPERTY OF <IOWA STATE UNIVERSITY>. ANY REPRODUCTION IN PART OR AS A WHOLE WITHOUT THE WRITTEN PERMISSION OF <IOWA STATE UNIVERSITY> IS PROHIBITED.
Dielectric Sensor
TITLE:
Rod Holder
SIZE
B
DWG. NO.
002-0008
REV
SCALE:2:1
WEIGHT:
SHEET 1 OF 1

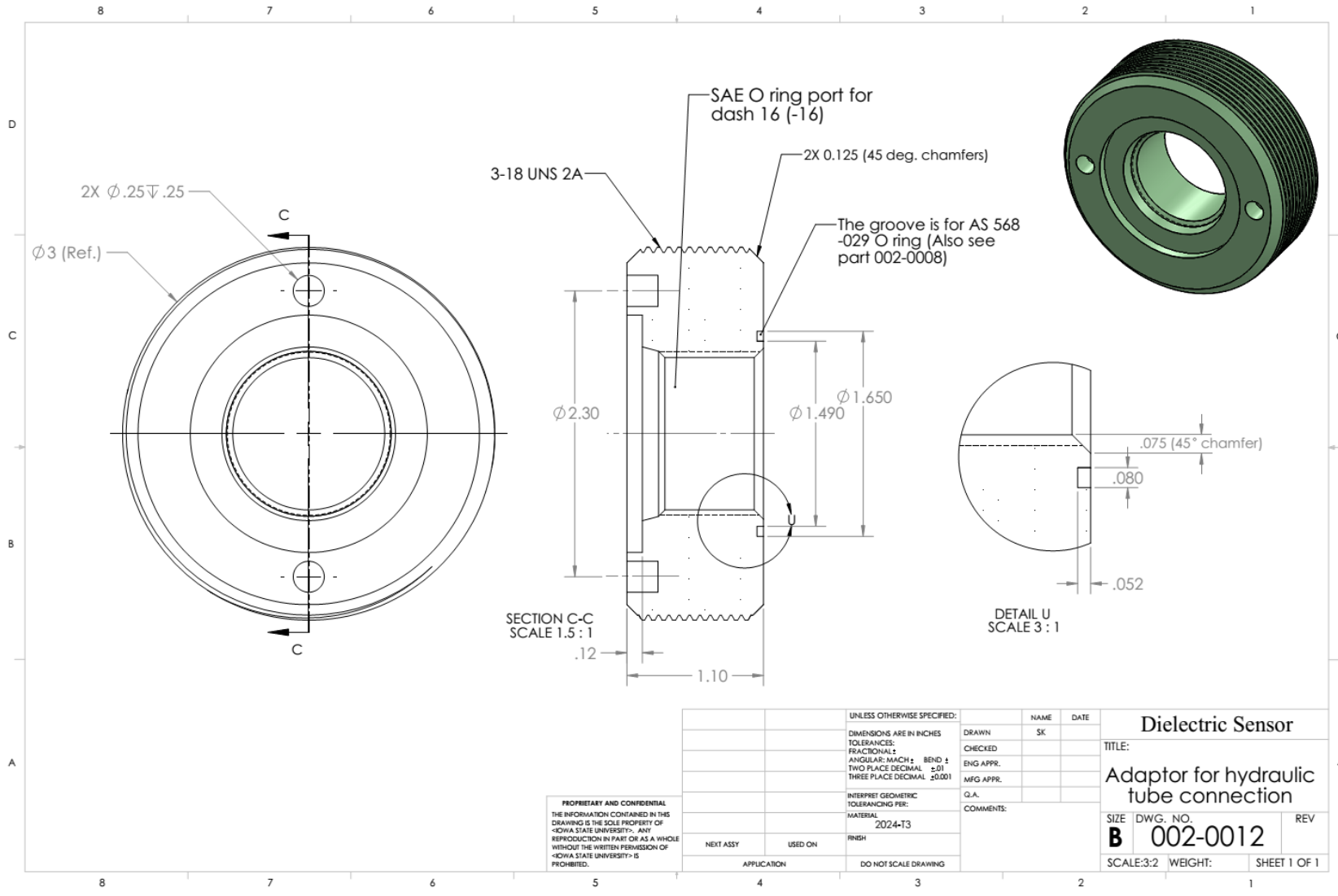

		UNLESS OTHERWISE SPECIFIED:		NAME	DATE
		DIMENSIONS ARE IN INCHES TOLERANCES: FRACTIONAL ± ANGULAR: MACH ± BEND ± TWO PLACE DECIMAL ±.01 THREE PLACE DECIMAL ±0.001	DRAWN	SK	
			CHECKED		
			ENG APPR.		
			MFG APPR.		
			Q.A.		
		INTERPRET GEOMETRIC TOLERANCING PER:	COMMENTS:		
		MATERIAL 2024-T3			
NEXT ASSY	USED ON	FINISH			
APPLICATION		DO NOT SCALE DRAWING			

Dielectric Sensor

TITLE:

Adaptor for hydraulic tube connection

SIZE	DWG. NO.	REV
B	002-0012	

SCALE:3:2 WEIGHT: SHEET 1 OF 1

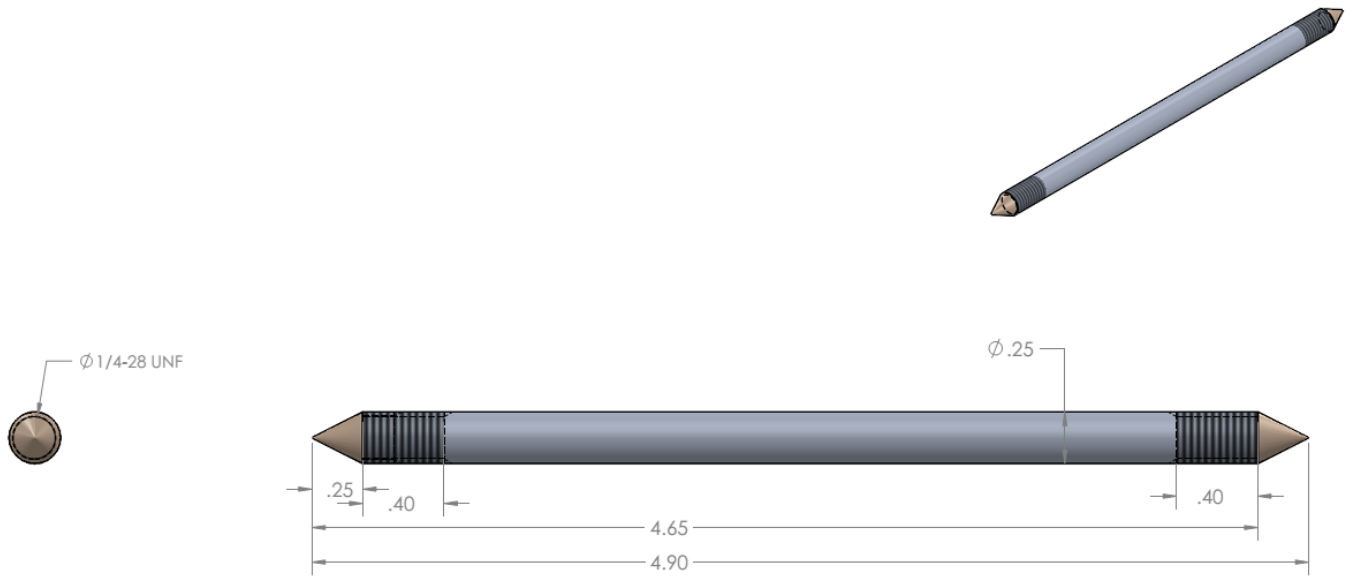

		UNLESS OTHERWISE SPECIFIED:		NAME	DATE
		DIMENSIONS ARE IN INCHES TOLERANCES: FRACTIONAL ± ANGULAR: MACH ± BEND ± TWO PLACE DECIMAL ±0.03 THREE PLACE DECIMAL ±	DRAWN	SK	
			CHECKED		
			ENG APPR.		
			MFG APPR.		
		INTERPRET GEOMETRIC TOLERANCING PER:	Q.A.		
		MATERIAL	COMMENTS:		
NEXT ASSY	USED ON	FINISH			
APPLICATION		DO NOT SCALE DRAWING			

Dielectric Sensor

TITLE: Central Electrode

SIZE	DWG. NO.	REV
B	002-0009	
SCALE: 1:8	WEIGHT:	SHEET 1 OF 1

Note : The dimensions and tolerances are based on part number 97395A441 (McMaster-Carr)

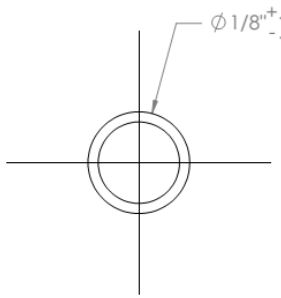

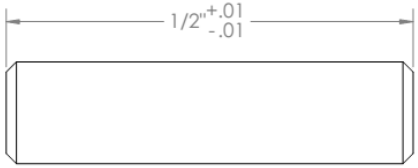

		UNLESS OTHERWISE SPECIFIED:		NAME	DATE
		DIMENSIONS ARE IN INCHES TOLERANCES: FRACTIONAL ± ANGULAR: MACH ± BEND ± TWO PLACE DECIMAL ± THREE PLACE DECIMAL ±	DRAWN	SK	
			CHECKED		
			ENG APPR.		
			MFG APPR.		
			Q.A.		
		INTERPRET GEOMETRIC TOLERANCING PER:	COMMENTS:		
		MATERIAL			
NEXT ASSY	USED ON	FINISH			
APPLICATION		DO NOT SCALE DRAWING			

Dielectric Sensor

TITLE:

SIZE	DWG. NO.	REV
B	003-0005	
SCALE: 1:8	WEIGHT:	SHEET 1 OF 1